

Geosphere

Early Miocene volcanic activity and paleoenvironment conditions recorded in tephra layers of the AND-2A core (southern McMurdo Sound, Antarctica).

--Manuscript Draft--

Manuscript Number:	GS754R2
Full Title:	Early Miocene volcanic activity and paleoenvironment conditions recorded in tephra layers of the AND-2A core (southern McMurdo Sound, Antarctica).
Short Title:	
Article Type:	Research Paper
Keywords:	Antarctica, volcanoclastic sediments, paleoenvironment, Mt. Morning, Victoria Land Basin
Corresponding Author:	Alessio Di Roberto, Ph.D. Istituto Nazionale di Geofisica e Vulcanologia Pisa, Italy ITALY
Corresponding Author Secondary Information:	
Corresponding Author's Institution:	Istituto Nazionale di Geofisica e Vulcanologia
Corresponding Author's Secondary Institution:	
First Author:	Alessio Di Roberto, Ph.D.
First Author Secondary Information:	
Order of Authors:	Alessio Di Roberto, Ph.D. Paola Del Carlo Sergio Rocchi Kurt Panter
Order of Authors Secondary Information:	
Abstract:	<p>The ANtarctic geological DRILLing program (ANDRILL) successfully recovered 1138.54 m of core from drillhole, AND-2A, in the Ross Sea sediments (Antarctica). The core is composed of terrigenous claystones, siltstones, sandstones, conglomerates, breccias, and diamictites with abundant volcanic material. In this work we present sedimentological, morphoscopic, petrographic, and geochemical data on pyroclasts recovered from core AND-2A, which provide insights on eruption styles, volcanic sources, and environments of deposition. One pyroclastic fall deposit, 12 resedimented volcanoclastic deposits and 14 volcanogenic sedimentary deposits record a history of intense explosive volcanic activity in southern Victoria Land during the Early Miocene. Tephra were ejected during Subplinian and Plinian eruptions fed by trachytic to rhyolitic magmas and during Strombolian to Hawaiian eruptions fed by basaltic to mugearitic magmas in submarine/subglacial to subaerial environments. The long-lived Mt. Morning eruptive centre, located c. 80 km south of the drillsite, was recognized as the probable volcanic source for these products on the basis of volcanological, geochemical, and age constraints. The study of tephra in the AND-2A core provides important paleoenvironment information by revealing that the deposition of primary and moderately reworked tephra occurred in a proglacial setting under generally open-water marine conditions.</p>

Cover Letter

[Click here to download Cover Letter: Letter to Editor.docx](#)

1 **Early Miocene volcanic activity and paleoenvironment conditions recorded in tephra layers of**
2 **the AND-2A core (southern McMurdo Sound, Antarctica).**

3
4 Di Roberto A.¹, Del Carlo P.¹, Rocchi S.², Panter K. S.³

5
6 1 Istituto Nazionale di Geofisica e Vulcanologia, Sezione di Pisa, via della Faggiola 32, I 56126
7 Pisa, Italy;

8 2 Dipartimento di Scienze della Terra, Università di Pisa, Via S. Maria, 53, I-56126 Pisa, Italy;

9 3 Department of Geology, Bowling Green State University, Bowling Green, OH, 43403, USA;

10

11 Keywords:

12 Antarctica

13 volcanoclastic sediments

14 paleoenvironment

15 Mt. Morning

16 Victoria Land Basin

17

18 **ABSTRACT**

19 The ANtarctic geological DRILLing program (ANDRILL) successfully recovered 1138.54 m of
20 core from drillhole, AND-2A, in the Ross Sea sediments (Antarctica). The core is composed of
21 terrigenous claystones, siltstones, sandstones, conglomerates, breccias, and diamictites with
22 abundant volcanic material. In this work we present sedimentological, morphoscopic, petrographic,
23 and geochemical data on pyroclasts recovered from core AND-2A, which provide insights on
24 eruption styles, volcanic sources, and environments of deposition. One pyroclastic fall deposit, 12
25 resedimented volcanoclastic deposits and 14 volcanogenic sedimentary deposits record a history of
26 intense explosive volcanic activity in southern Victoria Land during the Early Miocene. Tephra
27 were ejected during Subplinian and Plinian eruptions fed by trachytic to rhyolitic magmas and
28 during Strombolian to Hawaiian eruptions fed by basaltic to mugearitic magmas in
29 submarine/subglacial to subaerial environments. The long-lived Mt. Morning eruptive centre,
30 located c. 80 km south of the drillsite, was recognized as the probable volcanic source for these
31 products on the basis of volcanological, geochemical, and age constraints. The study of tephra in the
32 AND-2A core provides important paleoenvironment information by revealing that the deposition of
33 primary and moderately reworked tephra occurred in a proglacial setting under generally open-
34 water marine conditions.

35

36 **INTRODUCTION**

37

38 Over the last few decades significant insight on paleoenvironmental conditions in southern
39 Victoria Land have come from archives of sediments recovered in cores drilled both onshore and
40 offshore (Barrett et al., 1998 and 2000; Hambrey and Barrett, 1993; Fielding and Thomson, 1999;
41 Naish et al., 2007; Harwood et al., 2008). Recently, the ANtarctic geological DRILLing program
42 (ANDRILL) successfully recovered sediments and geophysical data from 1138.54 meters of drill-
43 core in the second AND-2A drill hole (southern McMurdo Sound; Florindo et al., 2008). The coring
44 site is located in the Ross Sea, approximately 50 km NW of Hut Point Peninsula on Ross Island
45 ($77^{\circ}45.488'S$; $165^{\circ}16.613'E$; Fig. 1).

46 The AND-2A core sampled an almost continuous (98% recovery) sequence of sediments
47 composed of lithologies including terrigenous claystones, siltstones, sandstones, conglomerates,
48 breccias, and diamictites (Florindo et al., 2008; Panter et al., 2008). Fourteen lithostratigraphic units
49 were identified on the basis of major changes in lithology recognized during core description
50 (Fielding et al., 2011). Sediments were interpreted to represent a wide and complex spectrum of
51 depositional environments and dynamic fluctuations in the Antarctic ice-sheet recorded in
52 numerous cycles of glacial advance and retreat during the Early to Middle Miocene (Fielding et al.,
53 2011; Passchier et al., 2011).

54 Results from $^{40}\text{Ar}/^{39}\text{Ar}$ radiometric dating of primary to moderately reworked tephra layers (Di
55 Vincenzo et al., 2010) range in age from Early Miocene to Pleistocene (c. 20 to c. 0.08 Ma) and
56 comprise an expanded and almost continuous section of Early to Middle Miocene sediments (c. 20
57 to c. 11.5 Ma), which has not been previously recorded by drilling in this region (Harwood et al.,
58 2009).

59 In this paper we present sedimentological, morphoscopic, petrographic and geochemical data
60 from tephra recovered in the AND-2A core. We also focus on some of the sedimentological aspects
61 of the tephra in order to infer their depositional history. The results provide constraints on volcanic
62 sources, eruptions styles and depositional paleoenvironments.

63

64 **THE EREBUS VOLCANIC PROVINCE**

65

66 The Erebus volcanic province in southern Victoria Land represents the largest area of exposed
67 late Cenozoic volcanic rocks and the most complete record of alkaline volcanism in Antarctica
68 (Kyle and Cole 1974; Kyle 1990a, b; Di Vincenzo et al., 2010). The Erebus volcanic province
69 comprises several large volcanic centers built on the western flank of the intracontinental West
70 Antarctic rift system in the McMurdo Sound region (Kyle, 1990b) that range in age from the Early
71 Miocene (c. 19 Ma) to the present day (Fig. 1). Ross Island is the largest volcanic complex in the
72 area and is formed by the active Mt. Erebus volcano, which is surrounded radially by the Mt.
73 Terror, Mt. Bird and Hut Point Peninsula eruptive centers. Mt. Erebus is composed mostly of

74 basanite and phonolite deposits (Kyle, 1977 and 1981; Kyle et al., 1992) that date back to 1.3 Ma
75 (basanite dyke from Cape Barne; Esser et al., 2004). Mt. Bird and Mt. Terror are basanitic shield
76 volcanoes that were active from 4.6 to 3.8 Ma and 1.7 to 1.3 Ma, respectively (Wright and Kyle,
77 1990a and b; Kyle and Muncy, 1989). Hut Point Peninsula is Pleistocene in age (c. 1.3 Ma) and
78 consists of alkaline volcanism that is dominated by basanitic-hawaiitic cinder cones and a phonolite
79 dome (Observation Hill) (Kyle, 1981).

80 To the south of Ross Island, the Erebus volcanic province is represented by White Island; a
81 basanite to tephriphonolite shield volcano that was active as early as 7.65 Ma (Cooper et al., 2007).
82 Recently, evidence for Late Miocene (c. 6.5 Ma) submarine to emergent volcanism was found in
83 close proximity to White Island (Di Roberto et al., 2010). Farther south, Black Island, Minna Bluff,
84 Mt. Morning and Mt. Discovery are all major eruptive centers belonging to Erebus volcanic
85 province. The Minna Bluff peninsula and Black Island volcanic complexes are both composed of
86 alkaline volcanic products belonging to the basanite-phonolite lineage and were active between c.
87 12 and 4 Ma (Fargo et al., 2008; Wilch et al., 2011) and between 11.2 and 1.7 Ma (Timms, 2006),
88 respectively. Mt. Morning is the oldest volcanic complex in the Erebus volcanic province and has
89 been divided into two phases of activity. Phase I (18.7 to 11.4 Ma) is dominated by mildly alkaline,
90 mostly trachytic rocks, and Phase II (6.13 to 0.02 Ma) is composed of strongly alkaline rocks
91 belonging to the basanite-phonolite lineage (Kyle and Muncy 1989; Wright and Kyle 1990c;
92 Wright-Grassham 1987; Kyle, 1990a and b; Paulsen and Wilson, 2009; Martin, 2009; Martin et al.,
93 2010).

94 North of Ross Island, Franklin and Beaufort islands represent remnants of alkaline volcanic
95 edifices, with ages that range from Quaternary (90 ± 66 ka; date from a seamount 10 km north of
96 Franklin Island) to Late Miocene (6.80 ± 0.05 Ma) (Rilling et al., 2009). In addition to the large
97 volcanic edifices, the Erebus volcanic province includes several small volcanic centers and fields
98 (Kyle and Cole, 1974; Kyle, 1990b). Numerous volcanic ash deposits are found within the hyper-
99 arid Dry Valleys region of the Transantarctic Mountains, chiefly in the Royal Society Range and the
100 Wright-Taylor Valleys. Most of these volcanoclastic deposits were reported to be Miocene to
101 Pliocene in age with $^{40}\text{Ar}/^{39}\text{Ar}$ ages ranging from c. 15.15 to c. 4.33 Ma (Kyle and Cole, 1974;
102 Kyle, 1990a; Marchant et al., 1996; Lewis et al., 2007). The Dailey Islands are c. 10 km south of the
103 SMS drillsite and consist of heavily eroded remnants of basaltic cinder cones and lava deposits.
104 Studies of volcanic rocks from two of the five islands reveal paleomagnetic normal polarities and
105 radiometric ages of 0.78 ± 0.04 Ma (Mankinen and Cox, 1988; Tauxe et al., 2004; Del Carlo et al.,
106 2009). Finally, traces of the earliest activity within the Erebus volcanic province comes from
107 volcanoclastic detritus and tephra recovered in the CIROS-1, MSSTS-1, Cape Roberts Project and
108 AND-2A drillcores, which extends the volcanic history of the province back to ~ 26 Ma (Gamble et
109 al., 1986; Barrett, 1987; McIntosh, 1998 and 2000; Acton et al., 2008; Di Vincenzo et al., 2010).

110

111 **VOLCANIC ROCKS IN AND-2A CORE AND ANALYTICAL METHODS**

112

113 Preliminary stratigraphic and petrologic data on volcanic products in the AND-2A core were
114 reported in Fielding et al. (2008) and Panter et al. (2008), and provide the foundation for this study.
115 The volcanic material in the AND-2A core includes dispersed clasts of lava, scoria fragments and
116 pumices, variably reworked tephra layers and one primary tephra. More than 50% of the total clasts
117 identified in 9 of the 14 lithostratigraphic units (LSU) are volcanic in origin and LSU 1 (0 to 37
118 meters below sea floor – m b.s.f) represents the most volcanic-rich unit within the core. The weakly
119 reworked tephra beds, lava breccias and ripple cross-laminated vitroclastic sands in LSU 1 are
120 interpreted to be deposited in a shallow marine environment by Strombolian- and Hawaiian-type
121 volcanism from proximal volcanic sources (Del Carlo et al., 2009).

122 For this study, 27 volcanoclastic beds were identified and sampled from LSU 2 to LSU 14 (i.e.
123 between 37.07 and 1138.54 m b.s.f; Table 1) and their sedimentological and volcanological
124 characteristics are the basis for the interpretations presented in this paper. Because most of these
125 samples are poorly lithified, they were impregnated with epoxy resin and prepared as standard
126 polished thin sections for petrography and electron microprobe analysis. Observations of the
127 sediments and sedimentary rocks were made using a stereomicroscope in order to detail
128 sedimentologic structures and qualitatively identify sediment components and their relative
129 abundance. This work led to the selection of samples for scanning electron microscopy and analysis
130 by electron microprobe. Morphological and textural observations of components were performed by
131 means of scanning electron microscopy (SEM) at Istituto Nazionale di Geofisica e Vulcanologia
132 (Sezione di Pisa) using a Zeiss EVO MA 10 equipped with an Oxford ISIS microanalysis system.
133 Major element glass composition and mineral analyses of glass-bearing volcanic fragments and
134 alteration phases were performed at the HPHT Laboratory of Istituto Nazionale di Geofisica e
135 Vulcanologia (Sezione di Roma) using a JEOL JXA 8200 microprobe equipped with 5 wavelength-
136 dispersive spectrometers (WDS) and an energy-dispersive analyzer system (EDS). Instrumental
137 conditions were: accelerating voltage 15 kV, beam current 5 nA, probe diameter 5 μm , acquisition
138 time 10 s and 5 s for peak and background, respectively. Whenever possible, a minimum of 25
139 particles were analyzed in each sample. Relative standard errors for each element are reported in
140 Supplemental Table 1.

141

142 **RESULTS**

143

144 The sampled deposits have been grouped into three types based on sedimentary features, the
145 nature and abundance of components (Figs. 2 and 3), and on the major element compositions of

146 glassy fragments (Fig. 5 and Table 2). They are: (i) pyroclastic fall deposits, (ii) resedimented
147 volcanoclastic deposits, and (iii) volcanogenic sedimentary deposits (terminology after McPhie et
148 al., 1993).

149

150 **Pyroclastic fall deposit**

151

152 A 6 cm-thick (640.13 and 640.19 m b.s.f) pyroclastic fall deposit was identified between within
153 LSU9 (Panter et al., 2008; Di Vincenzo et al., 2010). The lapilli tuff is massive to faintly normally
154 graded and contains a homogeneous distribution of pale green pumice fragments (<3 mm in
155 diameter) set in matrix formed by angular glass shards that range in size from coarse to very fine
156 ash. The lapilli tuff is under and overlain by volcanic-rich sandstones composed of light brown
157 fresh volcanic glass shards, pale green to white altered glass shards, abundant lithic fragments
158 (commonly of metasandstones and schists and less commonly of granite, dolerite and marble) and
159 loose crystals (mainly quartz, feldspars and plagioclase).

160 The contact with the underlying sediment is sharp whereas the upper contact is gradational (Fig.
161 2A). Pale green pumices are moderately to highly vesicular (Houghton and Wilson, 1989) with a
162 frothy morphology. Vesicles range in shape from spherical to elongated and are sometimes
163 deformed (collapsed) or highly coalesced. Pumices are mostly aphyric with rare, K-feldspar
164 phenocrysts (<2 mm), occasionally occurring with strongly green-colored clinopyroxene (<1 mm;
165 optically determined aegirine/aegirine-augite). Angular glass shards are usually blocky, vesicle-free
166 to poorly vesicular with vesicles ranging in shape from spherical to oblate (collapsed). A continuous
167 spectrum of vesicularity exists between vesicle-free glass shards and highly vesicular pumice. Glass
168 fragments forming the fine-grained part of the deposit (very fine ash) are variably vesicular
169 (analogous to those described above) and range in shape from y-shaped to cusped and blocky (Fig.
170 3A).

171 Most of the analyzed glass shards and pumice fragments are subtly to weakly altered with thin
172 (<3 μm) transparent rims of leached glass at the surface of the grains and along fractures and
173 vesicles (Fig. 3E). Well developed, pervasive perlitic fractures occur chiefly in dense, angular glass
174 fragments (Fig. 3F). The deposit is cemented by calcite and clay minerals.

175

176 **Resedimented volcanoclastic deposits**

177

178 Twelve resedimented volcanoclastic deposits (defined in accordance with McPhie et al., 1993)
179 were identified between 621.24 and 1093 m b.s.f (LSU9-13; Table 1). Two groups were
180 distinguished within these deposits: (i) resedimented pumice- and scoria-rich sandstone to
181 lapillistone (9 layers; Fig. 2B), and (ii) resedimented, strongly laminated, ash-rich mudstone to

182 sandstone (3 layers; Fig. 2C). Resedimented pumice- and scoria-rich sandstone to lapillistone
183 comprise grain-supported, <2 cm beds and lenses of pale green and clear, highly vesicular pumice
184 mixed with scoria clasts made up of variably vesicular (from dense to pumiceous), light to dark
185 yellow sideromelane and tachylite fragments (Fig. 3B). Clasts occur in a fine sand matrix, which is
186 cross- to parallel-laminated at mm to cm scale. The matrix is composed of glass fragments with the
187 same range of composition as the clasts, with crystals of K-feldspar, plagioclase, and quartz and
188 lithic fragments (metasandstones and schists and less commonly of granite, dolerite and marble;
189 Fig. 3B). Pumice and scoria fragments are in some cases abraded and subrounded. Deposits have
190 sharp and planar contacts with the underlying sediments whereas upper contacts are gradational to
191 diffuse; fragments with elongated shapes are commonly imbricated parallel to sand laminae or
192 oriented along the lee side of ripple cross-laminations. Pumice are similar in vesiculatity, alteration
193 degree (subtle to weak), and texture to those observed in the pyroclastic fallout deposit at 640.13-
194 640.19 m b.s.f (Fig. 3A); they are mostly aphyric with minor K-feldspar phenocrysts (<2 mm),
195 rarely accompanied by (<1 mm) strongly green-colored clinopyroxene (optically determined
196 aegirine/aegirine-augite). A second population of pumice and glass shards, showing textures similar
197 to those previously described but made of clear glass, was identified in five samples at 831.68,
198 953.28, 954.05, 1027.27 and 1093 m b.s.f, respectively, and rarely within sediments at shallower
199 depths. Scoria clasts and light to dark yellow sideromelane and tachylite fragments are pumiceous
200 to blocky to y-shaped (Figs. 2B and 3B). The scoria is weakly porphyritic with microphenocrysts of
201 plagioclase, rare strongly green-colored clinopyroxene and minor olivine, apatite and magnetite set
202 in a hypocrySTALLINE groundmass. Glass is pristine to subtly altered with rims of palagonite to
203 smectite a few microns-thick that line clasts or vesicles walls.

204 Resedimented, strongly laminated, ash-rich mudstone to sandstone consist of parallel laminated,
205 rhythmic couplets of grain-supported fine sandstone to siltstone grading upward to mudstone.
206 Couplets range in thickness from <1 mm to a few mm. Individual couplets have sharp lower and
207 upper contacts whereas internal contacts between the volcanoclastic silt/sand and clay facies range
208 from gradational to sharp (Figs. 2C and 3C). Volcanoclastic silt/fine sand laminae are composed of
209 pale green, highly vesicular pumice fragments mixed with dense to pumiceous, light brown-colored
210 sideromelane and tachylite fragments. Fragments are pristine and preserve thin vesicle glass walls
211 and fragile structures. Minor amounts of loose crystals (<1 mm) of K-feldspar, plagioclase and
212 quartz and lithics (commonly mafic lava fragments, granite dolerite and rarely schists) occur.
213 Lapilli-sized pumice fragments and sedimentary intraclasts (siltstone) occur and are observed to
214 load underlying clay laminae and be draped by laminae at the top.

215

216 **Volcanogenic sedimentary deposits**

217

218 Volcanogenic sedimentary deposits, namely shard-rich mudstones and sandstones (McPhie et al.,
219 1993), were identified at several depths (LSU2-13; Table 1). This type of deposit includes intervals
220 of < 2 mm, variably vesicular scoria, pale green and clear pumice set in sand to silt sized volcanic-
221 rich matrix. Abundant lithic fragments (Figs. 2D and 3D) of most commonly volcanic rocks are
222 recorded; they are mainly represented by variably vesicular lava with feldspar and < 2 mm, strongly
223 green-colored clinopyroxene (optically determined aegirine/aegirine-augite) set in an intergranular
224 to felted groundmass. Crystals of quartz, K-feldspar and biotite occur. Palagonitized glass shards
225 and vesicular fragments were found in some samples. Rare, holocrystalline intrusive rocks are
226 found that consist mainly of granitoids (quartz ± feldspar ± biotite ± hornblende) with
227 hypidiomorphic to allotriomorphic and moderately deformed textures. Rare metamorphic lithic
228 fragments were identified consisting of schist, gneiss, quartzite, and low-grade metasediments.
229 Bioclasts are common and include foraminifera, shell fragments, spicules, diatoms and bryozoans
230 (Fig. 3D). Irrespective of their origin (volcanic, metamorphic or biologic), fragments within vitric
231 siltstone and sandstone are usually sub- to well-rounded. Lithologies of lithic fragments are similar
232 to those of clasts described for the same interval by Panter et al. (2008) and Talarico et al. (2011)
233 and a more detailed description of their characteristics and inference on their provenance the reader
234 is referred to these papers.

235 Below 953.28 m b.s.f, the majority of glass fragments forming the volcanogenic sedimentary
236 deposits are moderately to strongly altered. Most of the original textures have been modified or
237 destroyed and volcanic glass is usually dissolved and replaced clay minerals, zeolites and
238 carbonates. In some samples “pseudo-fiamme” clasts are common and are interpreted to have
239 formed from burial compaction of lapilli-sized pumice clasts. Diffuse authigenic pyrite is found
240 together with framboidal agglomerates of microscopic (<1 µm) isometric crystals of greigite
241 (Fe₃S₄).

242

243 **Chemistry of volcanic glass**

244

245 A total of 600 glass fragments collected from throughout the length of the core have been
246 analyzed (Table 2 and Supplemental Figure 1). The SiO₂ contents of glass range from c. 40 to c.73
247 wt.% and have been divided into two main compositional groups: 1) light brown-colored
248 sideromelane and tachylite fragments with SiO₂ concentrations <52 wt.% and 2) pale green to
249 colourless glass fragments with SiO₂ >63 wt.%. The majority of glass fragments within the second
250 group are subtly to weakly altered and have low total oxides (<97 wt.%).

251 How the alteration effects the chemistry of volcanic glasses is examined semi-quantitatively by
252 plotting their compositions in the “Alteration box plot” (Large et al., 2001) shown in Figure 4. The
253 diagram combines the Alteration Index (AI) of Ishikawa et al. (1976) and the Chlorite-Carbonate-

254 Pyrite Index (CCPI) of Large et al. (2001) and was originally used with whole rock compositional
255 data in volcanic-hosted massive sulfide deposits to discriminate hydrothermal alteration mineral
256 assemblages from diagenetic assemblages. When used in combination with other compositional
257 data and detailed petrographic and textural observations, the "Alteration box plot" gives an
258 indication of alteration trends and processes.

259 Most of the low silica (52-63 wt.% SiO₂), light brown-colored sideromelane and tachylite
260 fragments found within all sediment types within the depth interval between 621.24 and 831.68 m
261 b.s.f. are pristine and plot within the least-altered rocks fields of the Alteration box plot (light blue
262 diamonds in Fig. 4). A few compositions are marked by a decrease of the CCPI values (depletion of
263 FeO + MgO versus Na₂O + K₂O; pink diamonds in Fig. 4) and likely indicate incipient
264 hydrothermal alteration. Below 831.68 m b.s.f., the alteration of light brown-colored sideromelane
265 and tachylite fragments increases further downcore with glass being progressively replaced by
266 zeolites and clay minerals and glass shards destroyed by compaction and diagenetic processes.

267 Throughout the core, the majority of the high silica (> 63 wt.% SiO₂), pale green to colorless
268 glass fragments is subtly to weakly altered. Above ~953 m b.s.f., the glasses show homogeneous AI
269 values ranging between ~40 and ~55, whereas values of CCPI vary more broadly between ~35 and
270 ~70 (red diamonds in Fig. 4). This indicates a rough increase of the CCPI values with respect to the
271 relatively least-altered rocks (depletion of Na₂O + K₂O versus FeO + MgO), which is typical of
272 hydrothermal alteration in the chlorite-dominated zone (Large et al., 2001). Below ~953 m b.s.f. to
273 the bottom of the core, glass compositions spread along the lower margin of the diagram having low
274 CCPI values (<20) and a wide range of AI values (~15 to 80; purple diamonds in Fig.4).

275 Most of the pale green to colorless glass fragments that were initially considered unaltered
276 (trachytic composition) plot across the lower margin of the Alteration Box Plot. Despite their high
277 total oxides (>97 wt. %) they are interpreted to be subtly based on the slight depletion in FeO +
278 MgO and variable depletion in Na₂O + K₂O + CaO (blue diamonds in Fig. 4).

279 The unaltered light brown-colored sideromelane and tachylite fragments range from basanite and
280 basalt/tephrite to mugearite and overlap compositions of other basic volcanic rocks from the Erebus
281 volcanic province (Fig. 5).

282 It is noteworthy that the pyroclastic fall deposit and resedimented volcanoclastic deposits have a
283 narrow range of AI and CCPI values, whereas the volcanogenic sedimentary deposits show a
284 broader range of values for these alteration indices. This could be attributed to the origin of each
285 deposit type. For instance, the pyroclastic fall deposit and resedimented volcanoclastic deposits are
286 considered to be composed of fragments emitted from the same source, transported together and
287 deposited contemporaneously. Alternatively, the volcanogenic sedimentary deposits maybe a
288 composite of products from multiple volcanic sources, with different transport and deposition
289 dynamics, and thus would should show greater variability in their degree of alteration.

290 Factors influencing the alteration of volcanic glass include the nature of the aluminosilicate
291 source material (e.g. glass vs. crystalline materials), the composition of original rock and of pore
292 fluids, pH and the temperature, and porosity of sediments. None of these factors seem to explain
293 why felsic glass shards dispersed within sediments are more altered than the coexisting basaltic
294 ones. Felsic glass is considered to alter at a slower rate relative to mafic glass. The alteration seems
295 to be related to the glass's viscosity, which in turn is a function of the composition and in particular
296 H₂O and SiO₂ content (Gifkins et al., 2005 and reference therein). A possible explanation for why
297 the basaltic glass is better preserved may be related to differences in the quenching (cooling) and
298 hydration history of mafic versus felsic magmas (Marsaglia and Tazaki, 1992). Felsic magmas
299 erupted in a water-rich environment (i.e. transitional or shallow water and subglacial) might have
300 hydrated and altered more quickly than basaltic glass emitted in a water free (subaerial)
301 environment.

302

303 **DISCUSSION**

304

305 **Eruptive styles**

306 Grain morphology, texture and vesicularity of pyroclasts are indicative of eruptive style and the
307 environment in which the eruption occurred. Magmatic eruptions typically produce variably
308 vesicular particles with cusped to frothy morphologies, determined by viscosity, temperature, and
309 volatile content (Cashman et al., 2000; Morrissey et al., 2000; Maria and Carey, 2002). Conversely
310 phreatomagmatic eruptions produce dense to poorly vesicular, often fine-grained (<100µm)
311 particles with a predominance of blocky morphologies (Cashman et al., 2000; Morrissey et al.,
312 2000; Maria and Carey, 2002). Primary volcanic particle morphology can then be affected by post-
313 eruptive reworking. Volcanic particles identified in the AND-2A core show a variety of
314 morphologies and range from vesicle free to highly vesicular, suggesting they were formed from
315 both magmatic and phreatomagmatic eruptions under a range of conditions, detailed below.

316

317 *High-silica glass*

318

319 The morphology and texture of highly vesicular pumice within the pyroclastic fall deposit and
320 resedimented volcanoclastic deposits in AND-2A core are indicative of magmatic fragmentation
321 processes. These products are emitted during energetic Subplinian and Plinian eruptions fed by
322 silicic magmas. During these eruptions large amounts of highly vesicular pumice (60-93 volume %;
323 Klug and Cashman, 1996; Cashman et al., 2000) and fine ashes are produced and carried in eruptive
324 columns up to several tens of kilometers-high and dispersed by winds distances up to hundreds of
325 kilometers from the source (Carey and Bursik, 2000).

326 In contrast, dense to poorly vesicular, fine-grained glass shards, with a predominance of blocky
327 morphologies, with hydration cracks and perlitic fracturing textures, suggest phreatomagmatic
328 fragmentation processes (Heiken and Wohletz, 1985 and 1991; Houghton and Wilson, 1989).
329 Phreatomagmatic eruptions may occur in sub-marine and sub-lacustrine environments, or when
330 magma comes into contact with groundwater or wet-sediment (Heiken and Fisher, 2000). In
331 glacial marine environments like McMurdo Sound the most likely water sources for phreatomagmatic
332 process are seawater and ice (Smellie, 2000).

333 Despite strong differences in morphology and vesicularity, the highly vesicular pumice and
334 dense to poorly vesicular glass fragments have the same chemical composition (and degree of
335 alteration) and coexist within the same layer, indicating that they may represent different
336 fragmentation processes (magmatic versus phreatomagmatic) within a single eruption. In addition,
337 as described above, a continuum between end member types which cover the whole spectrum of
338 vesicularity occur within these layers. This is consistent with a volcanic eruption occurring in a
339 transitional environment; i.e. evolving from shallow water or sub-glacial conditions (strong magma-
340 water interaction) to a subaerial environment (no magma-water interaction). Alternatively, multiple
341 vents located in subaerial and shallow subaqueous environments or a single vent experiencing rapid
342 cycling between 'dry' Strombolian and 'wet' phreatomagmatic explosions during a single eruptive
343 phase (Panter and Winter, 2008) may be invoked.

344

345 *Low-silica glass*

346

347 Sideromelane and tachylite fragments are frothy, blocky, y-shaped, or cusped and vary from
348 vesicle-free to highly vesicular. Most of the vesicular scoria observed are typical of weakly to
349 mildly explosive Strombolian or Hawaiian style eruptions (Cashman et al., 2000). Strombolian
350 eruptions consist of rhythmic, usually short-lived, mildly energetic explosions during which
351 magmatic volatiles are released and significant amounts of ash- to bomb- sized materials are ejected
352 to heights of a few hundred metres above a crater. Hawaiian style eruptions involve lava flows
353 together with lava fountains typically tens to hundreds of metres height. Typically lava fountains
354 are fed by basaltic magmas characterized by low viscosity, low volcanic gas content, and high
355 temperature. Lava fountains eject pyroclasts ranging in size from millimeters to about one metre in
356 diameter (Parfitt, 2004). Pyroclasts formed during Strombolian- and Hawaiian-style eruptions
357 accumulate mainly as coarse, primary fallout deposits within a few kilometers of the vent. Only in
358 the rare cases of strong magmatic fragmentation, for example during violent Strombolian or Plinian
359 basaltic eruptions, can pyroclasts be dispersed hundreds of kilometers from the source.

360 As with high-silica glasses , the presence of basaltic particles that are dense to poorly vesicular
361 and fine-grained with blocky morphologies in AND-2A pyroclastic fall and resedimented
362 volcanoclastic deposits may indicate phreatomagmatic activity.

363

364 **Volcanic source**

365

366 Major element compositions of glass fragments combined with $^{40}\text{Ar}/^{39}\text{Ar}$ age data from the
367 pyroclastic fall deposit and resedimented volcanoclastic deposits (see Table 1; age data from Di
368 Vincenzo et al. 2010) provide information on the provenance of volcanic materials. The ages of
369 studied AND-2A samples vary from c. 20 to 17.11 Ma (Early Miocene), according to $^{40}\text{Ar}/^{39}\text{Ar}$
370 age determinations of Di Vincenzo et al. (2010). Volcanic activity of comparable age occurred
371 on the Malta Plateau in the Melbourne volcanic province (Armienti et al., 1991; Müller et al.,
372 1991) and in the Erebus volcanic province at Mt. Morning (Kyle and Muncy, 1989; Wright and
373 Kyle, 1990c; Wright-Grassham, 1987; Kyle, 1990a and b; Martin et al., 2010). In the Melbourne
374 volcanic province, Middle Eocene magmatic activity is preserved in the form of multiple
375 intrusions dated at 47.5 and 38.6 Ma (Tonarini et al., 1997; Rocchi et al., 2002). The oldest
376 subaerial volcanic rocks crop out at Malta Plateau and Deception Plateau dated at c. 15 and 14
377 Ma (Armienti and Baroni, 1999). Dykes at Malta Plateau, possibly feeding lava flows, are dated
378 between c. 18.2 and 14.1 Ma (Schmidt-Thomé et al., 1990). Although similar in composition and
379 age, it is highly unlikely that Early to Middle Miocene volcanism in northern Victoria Land
380 (Malta Plateau) is the source for AND-2A deposits simply because this activity occurred over
381 500 km north of the drillsite and the predominate wind and ice paleo-directions are inferred to
382 have been in a northward direction in McMurdo Sound area (Sandroni and Talarico, 2006;
383 Talarico and Sandroni, 2011). More likely, the volcanic source was to the south of the drillsite.
384 The oldest Erebus volcanic province rocks crop out at Mt. Morning, where $^{40}\text{Ar}/^{39}\text{Ar}$ and K-Ar
385 ages indicate that activity occurred in two phases: the first one between at least 18.7 Ma and 11.4
386 Ma and the second one between 6.13 and 0.02 Ma (Paulsen and Wilson, 2009; Martin, 2009;
387 Martin et al., 2010). Evidence of volcanic activity pre-dating the onset of documented Mt.
388 Morning volcanism was found in volcanoclastic detritus and tephra beds recovered in CIROS-1,
389 MSSTS-1 and Cape Roberts (CRP) drillcores. The dates on these materials extend activity
390 within the Erebus volcanic province back to c. 26 Ma (Gamble et al., 1986; Barrett, 1987;
391 McIntosh, 1998 and 2000; Acton et al., 2008; Di Vincenzo et al., 2010). Volcanic activity older
392 than c. 19 Ma can be ascribed to either a proto-Mt. Morning volcano buried under the present-
393 day Mt. Morning edifice, or to an unknown volcanic centre, which has been eroded away or
394 buried (Martin et al., 2010).

395 In Figures 5 and 6, major element compositions of glass fragments from the AND-2A core are
396 compared with those of Early to Middle Miocene products sampled on land or in drillcores and
397 attributed to the Erebus volcanic province (Armienti et al., 1998 and 2001; Pompilio et al., 2001;
398 Kyle, 1981; Smellie, 1998). Only a limited number of glass compositions are available for
399 McMurdo volcanics and the majority of data is from whole rocks. Nevertheless, the available data
400 indicate that there is strong similarity between compositions of glass fragments in AND-2A core
401 and some compositions of glass shards from volcanoclastic detritus and tephra beds recovered in
402 CRP2/2A drillcores, which has already been attributed to the activity of the Erebus volcanic
403 province (Armienti et al., 1998 and 2001; Smellie, 1998) and most likely sourced from Mt.
404 Morning. Discrepancies in the FeO_{tot} content between CRP2/2A drillcores glasses and AND-2A
405 core glass may be caused by minor alteration of the latter as indicated by the Alteration Box plot
406 (Figs. 4 and 7).

407 According to Martin (2009) and Martin et al. (2010) only 7% of Mt. Morning Phase I products
408 sampled are mafic whereas the remainder are felsic, specifically trachyte (79%) and rhyolite (14 %)
409 in composition. Our work and ongoing studies on sediments from different depth intervals (Nyland,
410 2011) indicate that mafic glass is abundant throughout the AND-2A core. The fresh mafic glass
411 have alkali basalt, basanite, tephrite and (less commonly) mugearite compositions (Fig. 5),
412 overlapping those of McMurdo Volcanic Group igneous products (Fig. 5; Kyle, 1990a; Armienti et
413 al., 1998; Rocchi et al., 2002; Nardini et al., 2009). At depths greater than 600 m b.s.f. the SiO_2
414 content of glass increases with increasing depth (Fig. 7). Unaltered basaltic compositions occur
415 prevalently above ~800 m b.s.f; below this depth they are altered and replaced by clay minerals and
416 zeolites. Glass compositions below ~840 m b.s.f show a shift towards higher SiO_2 contents, with the
417 highest (c. 70 wt.%) occurring near the bottom of the core (Fig. 7).

418 Our results complement the findings of Martin (2009) and Martin et al. (2010), confirming the
419 bimodal compositions of Mt. Morning products. However, we found that the abundance of basaltic
420 glass in the AND-2A core to be much higher than the 7% estimated for Mt. Morning deposits. This
421 suggests that during the period corresponding to Phase I activity at Mt. Morning, volcanism fed by
422 mafic magmas was much more prevalent than previously documented in surface deposits. This
423 discrepancy may be explained by the premise that present-day exposures on Mt. Morning may not
424 be representative of all of the material erupted. It could well be that Miocene trachyte and rhyolite
425 deposits on Mt. Morning, consisting of remnants of domes and welded pyroclastic flows, were more
426 resistant to weathering and erosion than basaltic scoria or even basaltic lava flows.

427 On the basis of textural and geochemical information we can infer eruption dynamics and
428 sources. Given that almost all studied samples consist of particles produced by a combination of
429 subaerial and submarine/sub-glacial magmatic and phreatomagmatic explosive activity (i.e. highly
430 vesicular pumice, basaltic vesicular scoria, and vesicle-free blocky fragments), we suggest three

431 possible scenarios: (i) a single volcanic complex, set in a transitional environment (submarine/sub-
432 glacial to subaerial) erupting products with bimodal composition (basaltic and trachytic-rhyolitic);
433 (ii) two contemporaneously active volcanic complexes, both set in a transitional environment
434 (submarine/sub-glacial to subaerial) and fed separately by basaltic and trachytic-rhyolitic magmas;
435 (iii) multiple contemporaneously active volcanic vents located in a range of environments
436 (submarine/sub-glacial to subaerial) and fed by basaltic and trachytic-rhyolitic magmas.

437

438 **Paleoenvironment implications**

439

440 Volcaniclastic deposits are an important component of sedimentary successions and are valuable
441 paleoenvironmental indicators. In marine and glacial marine environments, pyroclastic fall deposits
442 may result from subaerial volcanic activity and particle settling through a water column or by direct
443 transformation of gas-supported pyroclastic flow into a water-saturated gravity flow (Schneider et
444 al., 2001). Primary volcaniclastic deposits can also originate from submarine volcanic activity
445 ranging in styles from explosive to effusive (White, 2000). Resedimented volcaniclastic deposits
446 may result from reworking and resedimentation of pyroclasts previously erupted on land (including
447 supra-glacial, en-glacial and sub-glacial debris) or on sea ice.

448 Volcanic detritus is persistent and abundant throughout the AND-2A core, representing the
449 dominant clast type in 9 of the 14 lithostratigraphic units (Panter et al., 2008). Apart from LSU1
450 (Del Carlo et al., 2009), volcanic material within the uppermost half of the core (to 608.35 m b.s.f)
451 consists mostly of lava, scoria and pumice clasts dispersed in coarse-grained deposits (e.g.,
452 conglomerate, diamictite) and reworked glass in sandstone, siltstone and mudstone. The absence of
453 pyroclastic fall deposits and resedimented volcaniclastic deposits in the upper part of the core may
454 be explained by a combination of: (i) source, type and intensity of volcanic activity, (ii) ice extent
455 and environmental conditions within the McMurdo Sound at the time of deposition or (iii) erosional
456 processes.

457 During the period between c. 17.1 and 11.5 Ma when sediments were being deposited in the
458 upper 600 m of the core (Di Vincenzo et al., 2010), volcanic activity in southern Victoria Land may
459 have been less energetic (limited areal dispersion of ejecta), thus resulting in the lack of any discrete
460 tephra beds at the coring site. Eruptions may have been prevalently submarine or sub-glacial and
461 characterized by a limited dispersal of pyroclasts, as typically occurs for these types of eruptions.
462 However, this hypothesis seems to be in contrast with the recent findings of Martin et al. (2010),
463 that showed the presence of an intense and predominantly subaerial volcanic activity producing lava
464 flows and pyroclastic deposits at Gandalf Ridge (18.7 ± 0.3 and 15.5 ± 0.5 Ma), Pinnacle Valley
465 (15.4 ± 0.1 and 13.0 ± 0.3 Ma) and Mason Spur (12.9 ± 0.1 and 11.4 ± 0.2 Ma) that are located ~80 km
466 from the coring site. In addition this also seems to be in conflict with findings of Marchant et al.

467 (1996) and Lewis et al. (2007), which have documented mafic to felsic ash layers in the Dry
468 Valleys that are dated between 11 and 15 Ma. An alternative explanation is that the presence of
469 thick ice-sheets in the Ross Sea embayment, with grounding lines located north of the present day
470 positions, could have hampered the direct delivery of wind-driven volcanic materials to the coring
471 site (ii. glacial paleoenvironmental conditions). Sedimentological and isotopic studies of
472 sedimentary records demonstrate that changes in paleoenvironmental conditions occurred between
473 c. 17.1 and 11.5 Ma (Zachos et al., 2008; Passchier et al., 2011) and these were accompanied by
474 strong ice sheet fluctuations with multiple cycles of advance and retreat, which could possibly have
475 allowed the deposition of pyroclastic fall deposit. Pyroclastic fall deposit and resedimented
476 volcanoclastic deposits may have been eroded during the deposition of massive, coarse-grained
477 deposits (diamictite and conglomerates) in sub-glacial to pro-glacial environments.

478 Volcanic material within the bottom half of the core, >600 m b.s.f., consists of dispersed
479 lava clasts, scoria fragments, pumice, one pyroclastic fall deposit and at least ten resedimented
480 volcanoclastic deposits. Products forming the 6 cm-thick lapilli tuff at 640 m b.s.f., which is dated at
481 17.4 Ma (Di Vincenzo et al., 2010), were most likely transported in an eruptive ash cloud and
482 deposited directly through the water column. This would only be possible if open marine or partly-
483 open marine conditions prevailed at the time (Fig. 8). Rounding and abrasion of dispersed pumice
484 and scoria indicate that they spent some time as floating rafts prior to sinking, or transported on the
485 seafloor prior to deposition, or have undergone weathering and re-sedimentation prior to their final
486 deposition (Fig. 8). Limited mixing with fragments from non-volcanic material and imbrication of
487 clast parallel to sand laminae or oriented along the lee side of ripple cross-laminations, suggest
488 deposition by low energy volcanoclastic bottom or turbidity currents. Resedimented pumice- and
489 scoria-rich sandstone to lapillistone can be considered indicators of open water conditions with
490 limited sea ice, similar to the pyroclastic fall deposit at c. 640 m b.s.f. Resedimented, strongly
491 laminated, ash-rich mudstone to sandstone found at ~636 and ~1027 m b.s.f are comparable with
492 deposits generated by suspension settling from ice-proximal, turbid, melt water plumes (Ó Cofaigh
493 et al., 2001 and references therein), observed in fjord environments, and more rarely, in high-
494 latitude open marine settings. The absence of grain rounding, the preservation of fragile structures,
495 and the low degree of post-eruptive sediment mixing with non-volcanic detritus all indicate that no
496 significant reworking has occurred. We suggest that these pyroclasts were transported in eruptive
497 columns, dispersed by wind onto the ice (glaciers) and finally released to the water column during
498 repeated melting events. We therefore conclude that deposition of resedimented, strongly laminated,
499 ash-rich mudstone to sandstone occurred in a pro-glacial setting with general open marine
500 conditions. Similar depositional and dispersal processes have long been suggested for modern
501 volcanogenic sediments in McMurdo Sound (Bentley, 1979; Barrett et al., 1983; Macpherson,
502 1987; Atkins and Dunbar, 2009).

503

504 **CONCLUSIONS**

505 The sedimentological, morphoscopic, petrological and geochemical study of pyroclasts
506 recovered in AND-2A core has provided information about their volcanic sources and eruptions
507 styles and new insights into their environment of deposition. One pyroclastic fall deposit and
508 several re-sedimented, volcanoclastic deposits recovered in AND-2A core record an intense and
509 recurrent history of volcanic activity in southern Victoria Land region during the Early Miocene.
510 Two main explosive eruptive styles and magma compositions were recognised. Subplinian and
511 Plinian eruptions involved trachytic to rhyolitic magmas, while Strombolian to Hawaiian eruptions
512 were fed by basaltic to mugearitic magmas. In both cases the occurrence of vesicle-free, blocky
513 fragments indicates that hydromagmatic fragmentation processes were caused by the interaction of
514 magmas with seawater and/or glacial meltwater within a glaci-marine environment. On the basis of
515 the available geochemical and chronological data and using volcanological constraints, we infer that
516 the proto-Mt. Morning and Mt. Morning volcanoes located south of the drillsite are the most likely
517 volcanic sources. Finally, the sedimentological features of the volcanic units are interpreted to
518 indicate that they were deposited in a pro-glacial setting with overall open-water marine conditions.

519

520 **ACKNOWLEDGMENTS**

521

522 The ANDRILL Program is a multinational collaboration between the Antarctic Programs of
523 Germany, Italy, New Zealand and the United States. Antarctica New Zealand is the project
524 operator, and has developed the drilling system in collaboration with Alex Pyne at Victoria
525 University of Wellington and Webster Drilling and Enterprises Ltd. Scientific studies are jointly
526 supported by the US National Science Foundation, NZ Foundation for Research Science and
527 Technology, Royal Society of New Zealand Marsden Fund, the Italian Antarctic Research Program,
528 the German Research Foundation (DFG) and the Alfred Wegener Institute for Polar and Marine
529 Research (Helmholtz Association of German Research Centers). Antarctica New Zealand supported
530 the drilling team at Scott Base; Raytheon Polar Services supported the science team at McMurdo
531 Station and the Crary Science and Engineering Laboratory. The ANDRILL Science Management
532 Office at the University of Nebraska-Lincoln provided science planning and operational support.
533 ADR benefited of a post-doc grant from PNRA. Authors are grateful to Co-Chiefs F. Florindo and
534 D. Harwood and the Science Team (<http://www.andrill.org>) of the SMS ANDRILL project. A.
535 Cavallo is kindly acknowledged for the assistance during microprobe analyses. S. Petrushak is
536 kindly acknowledged for collecting samples of AND-2A core at Antarctic Marine Research Facility

537 at Florida State University. A.P. Martin and anonymous reviewers are also acknowledged for their
538 accurate and critical revision of the manuscript.

539

540 **REFERENCES CITED**

541

542 Acton, G.; Crampton, J.; Di Vincenzo, G.; Fielding, Christopher R.; Florindo, F.; Hannah, M.;
543 Harwood, D. M.; Ishman, S.; Johnson, K.; Jovane, L.; Levy, Richard; Lum, B.; Marcano, M. C.;
544 Mukasa, S.; Ohneiser, C.; Olney, M. P.; Riesselman, C.; Sagnotti, L.; Stefano, C.; Strada, E.;
545 Taviani, M.; Tuzzi, E.; Verosub, K. L.; Wilson, G. S.; Zattin, M.; and ANDRILL-SMS Science
546 Team, 2008, Preliminary integrated chronostratigraphy of the AND-2A core, ANDRILL Southern
547 McMurdo Sound Project. *in* Harwood, D.M., Florindo, F., Talarico, F., Levy, R.H., eds., *Studies*
548 *from the ANDRILL, Southern McMurdo Sound Project, Antarctica: Terra Antartica*, v. 15, 211-
549 220.

550

551 Armienti, P., and Baroni, C., 1999, Cenozoic climatic change in Antarctica recorded by volcanic
552 activity and landscape evolution: *Geology*, v. 27, p. 617-620.

553

554 Armienti, P., Civetta, I., Innocenti, F., Manetti, P., Tripodo, A., Villari, L., and Vita, G., 1991, New
555 petrographical and geochemical data on Mt. Melbourne volcanic field, Northern Victoria Land,
556 Antarctica: *Memorie della Società Geologica Italiana*, v. 46, p. 397-424.

557

558 Armienti, P., Messiga, B. and Vannucci, R., 1998, Sand provenance from major and trace element
559 analyses of bulk rock and sand grains: *Terra Antartica*, v. 5, p. 589-599.

560

561 Armienti, P., Tamponi, M., and Pompilio, M., 2001, Petrology and provenance of volcanic clasts,
562 sand grains and tephra: *Terra Antartica*, v. 8, p. 2-23.

563

564 Armstrong, R.L., 1978, K-Ar dating: Late Cenozoic McMurdo Volcanic Group and Dry Valley
565 glacial history, Victoria Land, Antarctica: *New Zealand Journal of Geology and Geophysics*, v.
566 21, p. 685-698.

567

568 Armstrong, R.L., Hamilton, W., and Denton, G.H., 1968, Glaciation in Taylor Valley, Antarctica,
569 older than 2-7 million years, *Science*, v. 159, p. 187-188.

570

571 Atkins, C.B., and Dunbar, G.B., 2009, Aeolian sediment flux from sea ice into Southern McMurdo
572 Sound (SMS), *Antarctica: Global and Planetary Change*, v. 69, p. 133-141.
573

574 Barrett, P.J., 1987, Oligocene sequence cored at CIROS-1, western McMurdo Sound: *New Zealand*
575 *Antarctic Record*, v. 7, p. 1–17.
576

577 Barrett, P.J., Fielding, C.R., and Sherwood W., 1998, Initial report on CRP-1, Cape Roberts Project,
578 *Antarctica: Terra Antarctica*, v. 5(1), 187 p., hdl:10013/epic.28286.d001
579

580 Barrett, P.J., Pyne, A.R., and Macpherson, A.J., 1983, Observations of the sea floor of McMurdo
581 Sound and Granite Harbour: *New Zealand Antarctic Record*, v. 5, p. 16–22.
582

583 Barrett, P.J., Sarti, M, and Sherwood, W., 2000, Studies from the Cape Roberts Project, Ross Sea,
584 *Antarctica, Initial Reports on CRP-3: Terra Antarctica*, v. 7, 209 p.
585

586 Bentley, P.N., 1979, Characteristics and distribution of windblown sediment, Western McMurdo
587 Sound, *Antarctica*. [BSc. Hons Thesis]: Wellington, Victoria University of Wellington, New
588 Zealand.
589

590 Carey, S., and Bursik, M., 2000, Volcanic plumes, *in in* Sigurdsson, H., Houghton, B.F., McNutt,
591 S.R., Rymer, H., and Stix, J., eds., *Encyclopedia of Volcanoes: San Diego, U.S., Academic*
592 *Press*, p. 527-544.
593

594 Cashman, K.V., Sturtevant, B., Papale, P., and Navon, O., 2000, Magmatic fragmentation, *in*
595 *Sigurdsson, H., Houghton, B.F., McNutt, S.R., Rymer, H., and Stix, J., eds., Encyclopedia of*
596 *Volcanoes: San Diego, U.S., Academic Press*, p. 421-430.
597

598 Cooper, A.F., Adam, L.J., Coulter, R.F., Eby, G.N., and McIntosh, W.C., 2007, Geology,
599 geochronology and geochemistry of a basanitic volcano, White Island, Ross Sea, *Antarctica:*
600 *Journal of Volcanology and Geothermal Research*, v. 165, p. 189-216, doi:
601 10.1016/j.jvolgeores.2007.06.003.
602

603 Del Carlo, P., Panter, K.S., Bassett, K., Bracciali, L., Di Vincenzo, G., and Rocchi, S., 2009, The
604 upper lithostratigraphic unit of ANDRILL AND-2A core (Southern McMurdo Sound,
605 Antarctica): Local volcanic sources, paleoenvironmental implications and subsidence in the

606 western Victoria Land Basin: *Global and Planetary Change*, v. 69, p. 142-161, doi:
607 10.1016/j.gloplacha.2009.09.002.
608

609 Di Roberto, A., Pompilio, M., and Wilch, T.I., 2010, Late Miocene submarine volcanism in
610 ANDRILL AND-1B drill core, Ross Embayment, Antarctica: *Geosphere*, v. 6, p. 524-536, doi:
611 10.1130/GES00537.1.
612

613 Di Vincenzo, G., Bracciali, L., Del Carlo, P., Panter, K., and Rocchi, S., 2010, $^{40}\text{Ar}/^{39}\text{Ar}$ laser dating
614 of volcanogenic products from the AND-2A core (ANDRILL Southern McMurdo Sound
615 Project, Antarctica): *Bulletin of Volcanology*, v. 72, p. 487–505, doi: 10.1007/s00445-009-0337-
616 z.
617

618 Esser, R.P., Kyle, P.R., and McIntosh, W.C., 2004, $^{40}\text{Ar}/^{39}\text{Ar}$ dating of the eruptive history of Mt.
619 Erebus, Antarctica: *Volcano evolution: Bulletin of Volcanology*, v. 66, p. 671–686, doi:
620 10.1007/s00445-004-0354-x.
621

622 Fargo, A.J., McIntosh, W.C., Dunbar, N.W., and Wilch, T.I., 2008, $^{40}\text{Ar}/^{39}\text{Ar}$ geochronology of
623 Minna Bluff, Antarctica: Timing of mid-Miocene glacial erosional events within the Ross
624 Embayment [abs.] *Eos (Transactions, American Geophysical Union)*, v. 89(53), Fall Meeting
625 Supplement.
626

627 Fielding C.R., Browne, G.H., Field, B., Florindo, F., Harwood, D.M., Krissek, L.A., Levy, R.H.,
628 Panter, K.S., Passchier, S., Pekar, S.F., 2011, Sequence stratigraphy of the ANDRILL AND-2A
629 drillcore, Antarctica: A long-term, ice-proximal record of Early to Mid-Miocene climate, sea-
630 level and glacial dynamism: *Palaeogeography, Palaeoclimatology, Palaeoecology*, v. 305, p.
631 336-351, doi: 10.1016/j.palaeo.2011.03.026
632

633 Fielding, C.R. and Thomson, M.R.A., 1999, Studies from the Cape Roberts Project, Ross Sea
634 Antarctica, Initial Report on CRP-2/2A: *Terra Antarctica, Bremerhaven, PANGAEA*, 6 (1), 173
635 pp.
636

637 Florindo, F., Harwood, D., and Levy, R. 2008. ANDRILL's Success During the 4th International
638 Polar Year: *Scientific Drilling*, v. 6, p. 29-31. doi:10.2204/iodp.sd.6.03.2008.
639

640 Gamble, J.A., Barrett, P.J., and Adams, C.J., 1986, Basaltic clasts from Unit 8: *Bulletin of New*
641 *Zealand*, v. 237, p. 145-152.

642

643 Gifkins, C.C., Herrmann, W., and Large, R.R., 2005 editors, *Altered volcanic rocks: a guide to*
644 *description*. Centre for Ore Deposit Research, University of Tasmania. 275 pp.

645

646 Hambrey, M.J., and Barrett P.J., 1993, Cenozoic sedimentary and climatic record, Ross Sea region,
647 Antarctica, *in* Kennett, J.P., and Warnke, D.A., eds, *The Antarctic Paleoenvironment: A*
648 *Perspective on Global Change: Part Two*, Antarctic Research Series, v. 60, Washington, D.C,
649 American Geophysical Union, pp. 91–124, doi:10.1029/AR060p0091.

650

651 Harwood, D.M., Florindo, F., Talarico, F., Levy, R.H., editors, 2008, *Studies from the ANDRILL,*
652 *Southern McMurdo Sound Project*, Antarctica: Terra Antarctica, v. 15, 253 pp.

653

654 Harwood, D.M., Florindo, F., Talarico, F., Levy, R.H., Kuhn, G., Naish, T., Niessen, F., Powell, R.,
655 Pyne, A., and Wilson, G., 2009, Antarctic drilling recovers stratigraphic records from the
656 continental margin: *Eos* (Transactions, American Geophysical Union), v. 90, no. 11, p. 90-91,
657 doi: 10.1029/2009EO110002.

658

659 Heiken, G.H., and Fisher, R.V., 2000, Water and magma can mix - A history of the concepts of
660 hydrovolcanism (1819 - 1980), *in* Negendank, J.F.W. and Brüchmann, C., eds., *International*
661 *Maar Conference: Germany: Terra Nostra*, v. 6, p. 165-189.

662

663 Heiken, G.H., and Wohletz, K.H., 1985, *Volcanic ash*: Berkeley, U.S., University of California Press,
664 , CA. 245 pp.

665

666 Heiken G.H., and Wohletz, K, 1991, [Fragmentation processes in explosive volcanic eruptions](#). *in*
667 Fisher, R.V., and Smith, G., eds *Sedimentation in Volcanic Settings*: Society of Sedimentary
668 Geology Special Publication, v. 45, p. 19-26.

669

670 Houghton, B.F., and Wilson, C.J.N., 1989, A vesicularity index for pyroclastic deposits: *Bulletin of*
671 *Volcanology*, v. 51, p. 451-462.

672

673 Ishikawa, Y., Sawaguchi, T., Iwaya, S. and Horiuchi, M., 1976, Delineation of prospecting targets for
674 Kuroko deposits based on modes of volcanism of underlying dacite and alteration haloes: *Mining*
675 *Geology*, v. 26, p. 105-117.

676

677 Klug, C., and Cashman K.V., 1996, Permeability development in vesiculating magmas: implications
678 for fragmentation: *Bulletin of Volcanology*, v. 58, p. 87-100.
679

680 Kyle, P.R., 1977, Mineralogy and glass chemistry of recent volcanic ejecta from Mt. Erebus, Ross
681 Island, Antarctica: *New Zealand Journal of Geology and Geophysics*, v. 20, p. 1123-1146.
682

683 Kyle, P.R., 1981, Mineralogy and geochemistry of a basanite to phonolite sequence at Hut Point
684 Peninsula, Antarctica, based on core from Dry Valley Drilling Project Drillholes 1, 2 and 3:
685 *Journal of Petrology*, v. 22, p. 451-500.
686

687 Kyle, P.R., 1982, Volcanic geology of the Pleiades, Northern Victoria Land, Antarctica, *in* Craddock
688 C., ed., *Antarctic Geoscience: Madison, University of Wisconsin Press*, p. 747-754.
689

690 Kyle, P.R., 1990a, McMurdo Volcanic Group – Introduction. *in* LeMasurier, W.E., and Thomson,
691 J.W., eds., *Volcanoes of the Antarctic plate and southern oceans: American Geophysical Union,*
692 *Antarctic Research Series*, v. 48, p. 19-25
693

694 Kyle, P.R., 1990b, Erebus Volcanic Province - Summary. *in* LeMasurier, W.E., and Thomson, J.W.,
695 eds., *Volcanoes of the Antarctic plate and southern oceans: American Geophysical Union,*
696 *Antarctic Research Series*, v. 48, p. 81-35
697

698 Kyle, P.R., and Cole, J.W., 1974, Structural control of volcanism in the McMurdo Volcanic Group,
699 Antarctica: *Bulletin of Volcanology*, v. 38, p. 16-25.
700

701 Kyle, P.R., Moore, J.A., and Thirwall, M.F., 1992, Petrologic evolution of anorthoclase phonolite
702 lavas at Mt. Erebus, Ross Island, Antarctica: *Journal of Petrology*, v. 33, p. 849-875.
703

704 Kyle, P.R., and Muncy, H.L., 1989, Geology and geochronology of McMurdo Volcanic Group rocks
705 in the vicinity of Lake Morning, McMurdo Sound, Antarctica: *Antarctic Science*, v. 1, p. 345–
706 350, doi: 10.1017/S0954102089000520.
707

708 Large, R.R., Gemmell, J.B., Paulick, H., and Huston, D.L., 2001, The alteration box plot: a simple
709 approach to understanding the relationship between alteration mineralogy and lithogeochemistry
710 associated with volcanic-hosted massive sulfide deposits: *Economic Geology*, v. 96, p. 957–971.
711

712 LeMaitre, R.W., 1989, ed., A Classification of Igneous Rocks and Glossary of Terms: Blackwell
713 Science, 193 pp.
714

715 LeMasurier, W.E. and Thomson, J.W., eds., 1990, Volcanoes of the Antarctic Plate and Southern
716 Oceans: Washington, D.C., American Geophysical Union, Antarctic Research Series, v. 48, 512
717 pp.
718

719 Lewis, A.R., Marchant, D.R., Ashworth, A.C., Hemming, S.R. and Machlus, M.L., 2007, Major
720 middle Miocene global climate change: evidence from East Antarctica and the Transantarctic
721 Mountains: Geological Society of America Bulletin. doi:10.1130B26134.1.
722

723 Macpherson, A.J., 1987, The MacKay Glacier/Granite Harbour system (Ross Dependency,
724 Antarctica). A study in nearshore glacial marine sedimentation. [Thesis]: Wellington, Victoria
725 University of Wellington, New Zealand, 85 pp.
726

727 Mankinen, E.A., and Cox, A., 1988, Paleomagnetic investigation of some volcanic rocks from the
728 McMurdo volcanic province, Antarctica: Journal of Geophysical Research, v. 93, p. 599-612.
729

730 Marchant, D.R., Denton, G.H., Swisher III, C.C. and Potter, N. Jr., 1996, Late Cenozoic Antarctic
731 paleoclimate reconstructed from volcanic ashes in the Dry Valleys region of southern Victoria
732 Land: Geological Society of American Bulletin, v. 108, p. 181–194.
733

734 Maria, A., and S. Carey, 2002, Using fractal analysis to quantitatively characterize the shapes of
735 volcanic particles, Journal of Geophysical Research, v. 107, p. 2283-2300,
736 doi:10.1029/2001JB000822.
737

738 Marsaglia, K.M., and Tazaki, K., 1992, Diagenetic trends in Leg 126 sandstones *in* Proceedings of
739 the Ocean Drilling Program, Scientific Results: College Station, Texas A & M University, p.
740 125-138.
741

742 Martin, A.P., 2009, Mt. Morning, Antarctica: Geochemistry, geochronology, petrology, volcanology,
743 and oxygen fugacity of the rifted Antarctic lithosphere [PhD thesis]: Dunedin, University of
744 Otago,.
745

746 Martin, A., Cooper, A., and Dunlap, W., 2010, Geochronology of Mt. Morning, Antarctica: two-
747 phase evolution of a long-lived trachyte-basanite-phonolite eruptive center: *Bulletin of*
748 *Volcanology*, v. 72, p. 357-371, doi: 10.1007/s00445-009-0319-1.
749

750 Mayewski, P.A., 1975, Glacial geology and late Cenozoic history of the Transantarctic Mountains,
751 Antarctica: Institute of Polar Studies, Report N°. 56, Ohio State University.
752

753 McIntosh, W.C., 1998, $^{40}\text{Ar}/^{39}\text{Ar}$ geochronology of volcanic clasts and pumice in CRP-1 core, Cape
754 Roberts, Antarctica: *Terra Antarctica*, v. 5, p. 683-690.
755

756 McIntosh, W.C., 2000, $^{40}\text{Ar}-^{39}\text{Ar}$ geochronology of tephra and volcanic clasts in CRP-2A, Victoria
757 Land Basin, Antarctica: *Terra Antarctica*, v. 7, p. 621-630.
758

759 McKelvey, B.C., Webb, P.N., Harwood, D.M. and Mabin, M.C.G., 1991, The Dominion Range
760 Sirius Group: a record of the late Pliocene–early Pleistocene Beardmore Glacier, *in* Thomson,
761 M.R.A., Crame, J.A., and Thomson, J.W., eds., *Geological Evolution of Antarctica*: Cambridge
762 University Press, p. 675-682.
763

764 McPhie, J., Doyle, M., Allen, R.L., editors 1993, *Volcanic Textures: A guide to the interpretation of*
765 *textures in volcanic rocks*: University of Tasmania, Centre for Ore Deposit and Exploration
766 Studies, 198 pp.
767

768 Mercer, J.H., 1968, Glacial geology of the Reedy glacier area, Antarctica: *Geological Society of*
769 *American Bulletin*, v. 79, p. 471-486.
770

771 Morrissey, M., Zimanowski, B., Wohletz, K., Buettner, R., 2000, Phreatomagmatic fragmentation, *in*
772 Sigurdsson, H., Houghton, B.F., McNutt, S.R., Rymer, H., and Stix, J., eds., *Encyclopedia of*
773 *Volcanoes*: San Diego, Academic Press, p. 231-245.
774

775 Müller, P., Schmidt-Thomé, M., Kreuzer, H., Tessensohn, F. and Vetter U., 1991, Cenozoic
776 peralkaline magmatism at the western margin of the Ross Sea, Antarctica: *Memorie della Società*
777 *Geologica Italiana*, v. 46, p. 315-336.
778

779 Muncy, H.L., 1979, Geologic history and petrogenesis of alkaline volcanic rocks, Mt. Morning,
780 Antarctica [Thesis]: Ohio State University, 224 pp.
781

782 Naish T., Powell R. and Levy R. H., editors, 2007, Studies from the ANDRILL, McMurdo Ice Shelf
783 Project, Antarctica – Initial Science Report on AND-1B: Terra Antarctica, 14, 328 pp.
784

785 Nardini, I, Armienti, P., Rocchi, S., Dallai, L., and Harrison, D., 2009, Sr-Nd-Pb-He-O isotope and
786 geochemical constraints on the genesis of cenozoic magmas from the West Antarctic Rift:
787 Journal of Petrology, v. 50, p. 1359-1375.
788

789 Nyland, R., 2011, Evidence for early-phase explosive basaltic volcanism at Mt. Morning from glass-
790 rich sediments in the ANDRILL AND-2A core and possible response to glacial cyclicity [MSc
791 Thesis]: Bowling Green State University, USA.

792

793 Ó Cofaigh, C., and Dowdeswell, J.A., 2001, Laminated sediments in glacimarine environments:
794 Diagnostic criteria for their interpretation: Quaternary Science Reviews, v. 20, p. 1411-436.
795

796 Panter, K.S., Talarico, F., Bassett, K., Del Carlo, P., Field, B., Frank, T., Hoffman, S., Kuhn, G.,
797 Reichelt, L., Sandroni, S., Tavini, M., Bracciali, L., Cornamusini, G., von Eynatten, H., and
798 Rocchi, R., 2008, Petrologic and geochemical composition of the AND-2A core, ANDRILL
799 Southern McMurdo Sound Project, Antarctica, in Harwood, D.M., Florindo, F., Talarico, F., and
800 Levy, R.H., eds., Studies from the ANDRILL, Southern McMurdo Sound Project, Antarctica:
801 Terra Antarctica, v. 15, p. 147-192.
802

803 Panter, K.S. and Winter, B., 2008, Geology of the side crater of the Erebus volcano, Antarctica:
804 Journal of Volcanology and Geothermal Research, v. 177, p. 578-588.
805

806 Parfitt, E.A., 2004, A discussion of the mechanisms of explosive basaltic eruptions: Journal of
807 Volcanology and Geothermal Research, v. 134, p. 77–107.
808

809 Passchier, S., Browne, G., Field, B., Fielding, C.R., Krissek, L.A., Panter, K., Pekar, S.F., and
810 ANDRILL-SMS Science Team, 2011, Early and middle Miocene Antarctic glacial history from
811 the sedimentary facies distribution in the AND-2A drill hole, Ross Sea, Antarctica: Geological
812 Society of America Bulletin, doi:10.1130/B30334.1.
813

814 Paulsen, T.S. and Wilson T.J., 2009, Structure and age of volcanic fissures on Mount Morning: A
815 new constraint on Neogene to contemporary stress in the West Antarctic Rift, southern Victoria

816 Land, Antarctica, Geological Society of America Bulletin, v. 121. p. 1071-1088; doi:
817 10.1130/B26333.1.
818

819 Pompilio, M., Armienti, P., and Tamponi, M., 2001, Petrography, Mineral Composition and
820 Geochemistry of Volcanic and Subvolcanic Rocks of CRP-3, Victoria Land Basin, Antarctica:
821 Terra Antarctica, v. 8, p. 469-480.
822

823 Rilling, S., Mukasa, S., Wilson, T., Lawver, L., and Hall C., 2009, New determinations of $^{40}\text{Ar}/^{39}\text{Ar}$
824 isotopic ages and flow volumes for Cenozoic volcanism in the Terror Rift, Ross Sea, Antarctica:
825 Journal of Geophysical Research, v. 114, doi:10.1029/2009JB006303.
826

827 Rocchi, S., Armienti, P., D'Orazio, M., Tonarini, S., Wijbrans, J.R. and Di Vincenzo, G., 2002,
828 Cenozoic magmatism in the western Ross Embayment: Role of mantle plume versus plate
829 dynamics in the development of the West Antarctic Rift System: Journal of Geophysical
830 Research, v. 107 , 10.1029/2001JB000515.
831

832 Sandroni, S., and Talarico, F.M., 2006, Analysis of clast lithologies from CIROS-2 core, New
833 Harbour, Antarctica-Implications for ice flow directions during Plio-Pleistocene time:
834 Palaeogeography, Palaeoclimatology, Palaeoecology, v. 231, p. 215-232.
835

836 Schmidt-Thomé, M., Mueller, P., and Tessensohn, F., 1990, McMurdo Volcanic Group-western Ross
837 Embayment: Malta Plateau: Antarctic Research Service, v. 48, p. 53-59.
838

839 Schneider, J.L., Le Ruyet, A., Chanier, F., Buret, C., Ferriere, J., Proust, J.N., and Rosseel, J.B, P.,
840 2001, Primary or secondary distal volcanoclastic turbidites: how to make the distinction? An
841 example from the Miocene of New Zealand (Mahia Peninsula, North Island), Sedimentary
842 Geology, v. 145, p. 1-22, doi: 10.1016/S0037-0738(01)00108-7.
843

844 Smellie, J.L., 1998, Sand grain detrital modes in CRP-1: provenance variations and influence of
845 Miocene eruptions on the marine record in the McMurdo Sound region: Terra Antarctica, v. 5, p.
846 579-587.
847

848 Smellie, J.L., 2000, Subglacial eruptions. *in* Sigurdsson, H., Houghton, B., Rymer, H., Stix, J., and
849 McNutt, S., eds., Encyclopedia of Volcanoes, San Diego, U.S., Academic Press, p. 403-418.
850

- 851 Talarico, F., Pace, D., and Sandroni, S., 2011, Amphibole-bearing metamorphic clasts in ANDRILL
852 AND-2A core: A provenance tool to unravel the Miocene glacial history in the Ross Embayment
853 (western Ross Sea, Antarctica): *Geosphere*, v. 7, p. 922-937, doi: 10.1130/GES00653.1.
854
- 855 Talarico, F., and Sandroni, S., 2011, Early Miocene basement clasts in ANDRILL AND-2A core and
856 their implications for paleoenvironmental changes in the McMurdo Sound region (western Ross
857 Sea, Antarctica): *Global and Planetary Change*, v. 78, p. 23-35,
858 doi:10.1016/j.gloplacha.2011.05.002.
859
- 860 Tauxe, L., Gans, P., and Mankinen, E.A., 2004, Paleomagnetism and ^{40}Ar - ^{39}Ar ages from volcanics
861 extruded during the Matuyama and Brunhes Chrons near McMurdo Sound, Antarctica:
862 *Geochemistry, Geophysics, Geosystems (G3)*, v. 5, doi:10.1029/2003GC000656.
863
- 864 Timms, C., 2006, Reconstruction of a grounded ice sheet in McMurdo Sound - evidence from
865 southern Black Island, Antarctica [MSc Thesis] Dunedin, University of Otago, 146 pp.
866
- 867 Tonarini, S., Rocchi, S., Armienti, P., and Innocenti, F., 1997, Constraints on timing of Ross Sea
868 rifting inferred from Cenozoic intrusions from northern Victoria Land, Antarctica, *in* Ricci, C.A.,
869 ed., *The Antarctic Region: Geological Evolution and Processes*, p. 511-521.
870
- 871 White, J.D.L., 2000, Subaqueous eruption-fed density currents and their deposits: *Precambrian*
872 *Research*, v., 101, p. 87-109
873
- 874 Wilch, T.I., Lux, D.R., Denton, G.H., and McIntosh, W.C., 1993, Minimal Pliocene–Pleistocene
875 uplift of the dry valleys sector of the Transantarctic Mountains: a key parameter in ice-sheet
876 reconstructions: *Geology*, v. 21, p. 841-844.
877
- 878 Wilch, T.I., McIntosh, W.C., Panter, K.S., Dunbar, N.W., Smellie, J.L., Fargo, A., Scanlan, M.,
879 Zimmerer, M.J., Ross, J., and Bosket, M.E., 2008, Volcanic and glacial geology of the Miocene
880 Minna Bluff Volcanic Complex, Antarctica: [abstract] *Eos (Transactions, American Geophysical*
881 *Union)*, v. 89, Fall Meeting Supplement, abs.V11F–06.
882
- 883 Wilch, T.I., Panter, K.S., McIntosh, W.C., Dunbar, N.W., Smellie, J.L., Fargo, A., Ross, J., Antibus,
884 J., Scanlan, M., Zimmerer, M., 2011. Miocene evolution of the Minna Bluff Volcanic Complex,
885 Ross Embayment, Antarctica. *International Symposium on Antarctic Earth Science XI*,
886 Edinburgh, Scotland, July 10-15. Abstract PS5.10.

887

888 Wright, A.C., and Kyle, P.R., 1990a, Mt. Bird, *in* LeMasurier, W.E., and Thomson, J.W., eds.,
889 Volcanoes of the Antarctic plate and southern oceans: American Geophysical Union Antarctic
890 Research Series, v. 48, p. 97–98.

891

892 Wright, A.C., and Kyle, P.R., 1990b, Mt. Terror, *in* LeMasurier, W.E., and Thomson, J.W., eds.,
893 Volcanoes of the Antarctic plate and southern oceans: American Geophysical Union Antarctic
894 Research Series, v. 48, p. 99–102.

895

896 Wright, A.C., and Kyle P.R., 1990c, Mount Morning, *in* LeMasurier, W.E., and Thomson, J.W., eds.,
897 Volcanoes of the Antarctic plate and southern oceans: American Geophysical Union Antarctic
898 Research Series, v. 48, p. 124–126.

899

900 Wright, A.C., and Kyle P.R., 1990d, Mason Spur, *in* LeMasurier, W.E., and Thomson, J.W., eds.,
901 Volcanoes of the Antarctic plate and southern oceans: American Geophysical Union Antarctic
902 Research Series, v. 48, p. 128–130.

903

904 Wright-Grassham, A.C., 1987, Volcanic geology, mineralogy and petrogenesis of the Discovery
905 volcanic subprovince, southern Victoria Land, Antarctica [Ph.D. Thesis]: New Mexico Institute
906 of Mining and technology. 460 pp. Unpublished.

907

908 Zachos, J.C., Dickens, G.R., and Zeebe, R.E., 2008, An early Cenozoic perspective on greenhouse
909 warming and carbon-cycle dynamics: *Nature*, v. 451, p. 279-283.

910

911 **Figures**

912 Figure 1. Map of southern Victoria Land, Antarctica, showing the location of AND-2A Southern
913 McMurdo Sound (SMS) core site and relevant geological features of Erebus Volcanic Province.
914 Map also shows outcrops of volcanic rocks (in dark brown) belonging to the McMurdo Volcanic
915 Group with relative time span of activity according to K-Ar and ^{40}Ar - ^{39}Ar ages (Mercer, 1968; Kyle
916 and Cole, 1974; Mayewski, 1975; Armstrong, 1978; Kyle, 1981, 1982, and 1990a,b; Kyle and
917 Muncy, 1989; Wright and Kyle, 1990a, b; McKelvey et al., 1991; Wilch et al., 1993; Marchant et
918 al., 1996; Esser et al., 2004; Tauxe et al. 2004; Timms, 2006; Cooper et al., 2007; Lewis et al.,
919 2007; Wilch et al., 2008; Paulsen and Wilson, 2009; Martin et al., 2010).

920

921 Figure 2. Core (left column) and thin section optical microscope images (right column)
922 representative of the four main volcanoclastic sediment types identified in AND-2A core: A and A₁)

923 pyroclastic fall deposit (640.13 m b.s.f), B and B₁) resedimented pumice- and scoria-rich sandstone
924 to lapillistone (709.13 m b.s.f.), C and C₁) resedimented, strongly laminated, ash-rich mudstone to
925 sandstone (636.23 m b.s.f.) and D and D₁) shard-rich mudstones and sandstones (712.04 m b.s.f.).
926 Dg = dense glass; lf = lava fragment; p = pumice; san = sanidine; sd = sideromelane.

927
928 Figure 3. Scanning electron microscope backscattered images representative of the four main
929 volcanoclastic sediment types identified in AND-2A core: A) pyroclastic fall deposit (dg = dense
930 glass; p = pumice), B) resedimented pumice- and scoria-rich sandstone to lapillistone, C)
931 resedimented, strongly laminated, ash-rich mudstone to sandstone and D) shard-rich mudstones and
932 sandstones. Bio = bioclast; dg = dense glass; lf = lava fragment; p = pumice; qz = quartz; san =
933 sanidine; sd = sideromelane. E) rims of leached glass occurring at the surface of the grains, along
934 fractures and vesicles; F) pervasive perlitic fractures occurring chiefly in glass shards and in the
935 least vesicular fragments.

936
937 Figure 4. AI–CCPI “Alteration box plot” diagram from Large et al. (2001) for analyzed AND-2A
938 glass fragments. Data show different degrees and styles of alteration within studied samples.
939 Colored rectangles identify least altered ‘boxes’ for unaltered rocks with <52 wt.% SiO₂, 52-63
940 wt.% SiO₂, 63-69 wt.% SiO₂ and >69 wt.% SiO₂, respectively. Full and open symbols respectively
941 represent the composition of unaltered glass and altered glass within the same sample.

942
943 Figure 5. Total Alkali versus Silica diagrams (TAS) from LeMaitre (1989) for unaltered AND-2A
944 glass compositions (blue diamonds). For comparison between composition of glasses in AND-2A
945 and Erebus volcanic province products (red dashed curve; Armienti et al., 1998 and references
946 therein), glass composition of fragment recovered in CRP1 (black crosses), 2/2A (black open
947 squares; Armienti et al., 1998; Armienti et al., 2001), volcanic products of the Phase I activity of
948 Mt. Morning (black open circles; Martin et al., 2010) and Mt. Morning volcanic rocks (pale red
949 open squares; Muncy, 1979; Wright-Grassham, 1987; Martin et al., 2010) are also reported.

950
951 Figure 6. Harker’s diagrams for unaltered AND-2A glass shards (blue diamonds). Glass
952 compositions are compared with the compositions of glass fragments recovered in CRP1 (black
953 crosses), 2/2a drillcores (black open squares) and attributed to proto-Mt. Morning and Mt. Morning
954 activity (Armienti et al., 1998; Armienti et al., 2001). Whole rock composition of Mt. Morning
955 volcanic rocks (Muncy, 1979; Wright-Grassham, 1987; Martin et al., 2010) are also reported (pale
956 red open squares)

957

958 Figure 7. SiO₂ vs. sample depth diagram. The diagram indicates a general correlation between depth
959 and the SiO₂ content of glasses (reconstructed compositions): altered rhyolitic-trachytic
960 compositions occur prevalently above 709.19 m b.s.f. whereas sample at 831.68 m b.s.f. marks the
961 passage towards rhyolitic glass compositions occurring between 953.28 m b.s.f. and core base.
962

963 Figure 8. Schematic model illustrating possible eruptive, transport, and depositional processes of
964 pyroclastic fall deposit, resedimented volcanoclastic deposits and the volcanogenic sedimentary
965 deposits. A) pyroclasts transported by a high eruptive column and finally deposited as pyroclastic
966 fall deposit directly through the water column in open water conditions; B) pumice and scoria clasts
967 windblown over the ice and resedimented by suspension settling from ice-proximal turbid
968 meltwater plumes or by low energy volcanoclastic bottom/turbidity currents (resedimented
969 volcanoclastic deposits); C) volcanic detritus deposited by glaci-marine processes (volcanogenic
970 sedimentary deposits).

971

972 Table 1. Descriptions of lithology and age data for pyroclastic fall deposit, resedimented
973 volcanoclastic deposits and volcanogenic sedimentary deposits analyzed in AND-2A core.

974

975 Table 2. Major elements chemical composition of unaltered glasses within AND-2A core of
976 pyroclastic fall deposit, resedimented volcanoclastic deposits and volcanogenic sedimentary deposits
977 (expressed as oxides weight %). The maximum and minimum values of SiO₂ wt.% are reported for
978 each sample. Chemical compositions of samples at 627.46-48 and 954.05-08 m b.s.f. were not
979 reported since they are entirely formed by altered glass shards.

980

Figure 1
[Click here to download high resolution image](#)

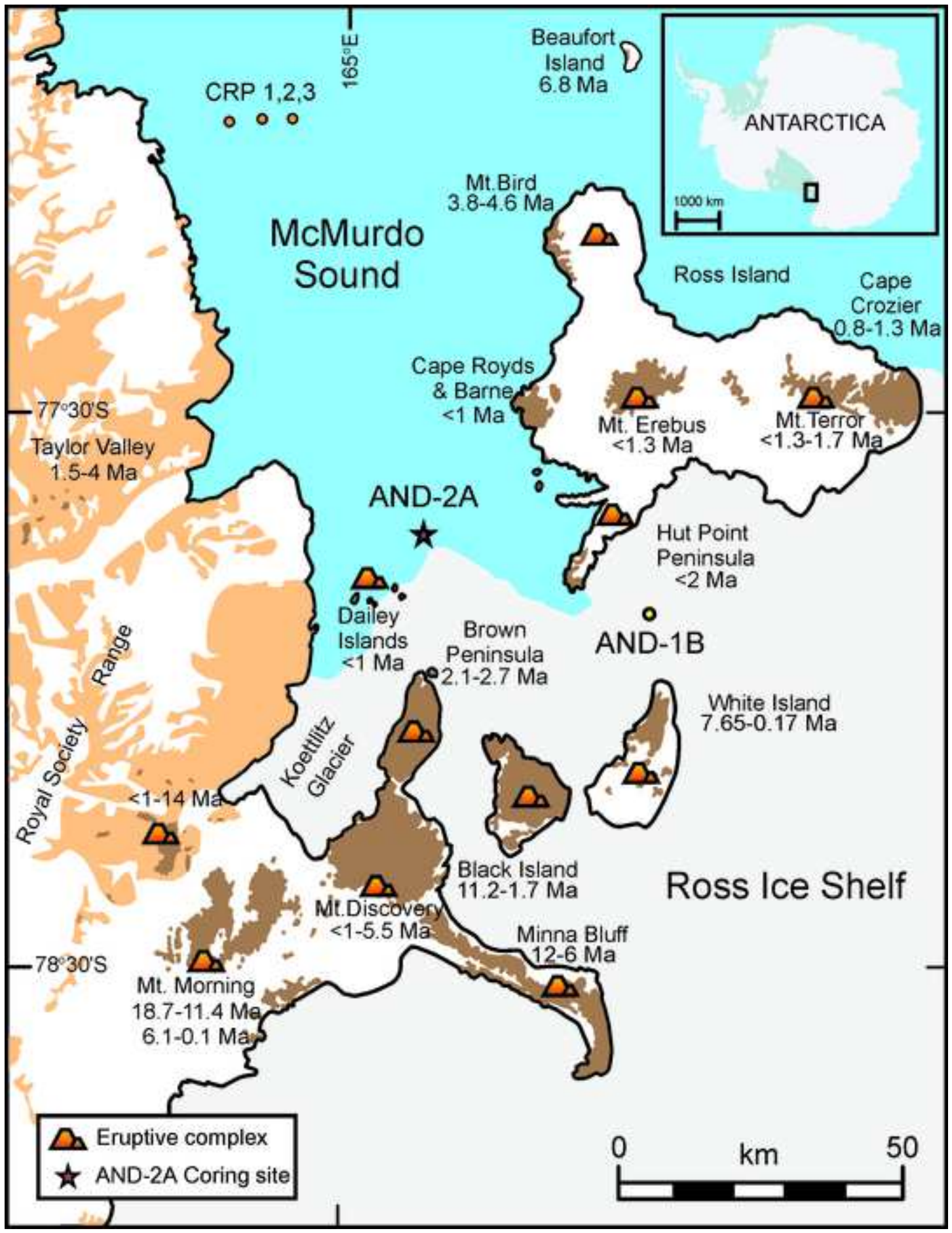


Figure 2
[Click here to download high resolution image](#)

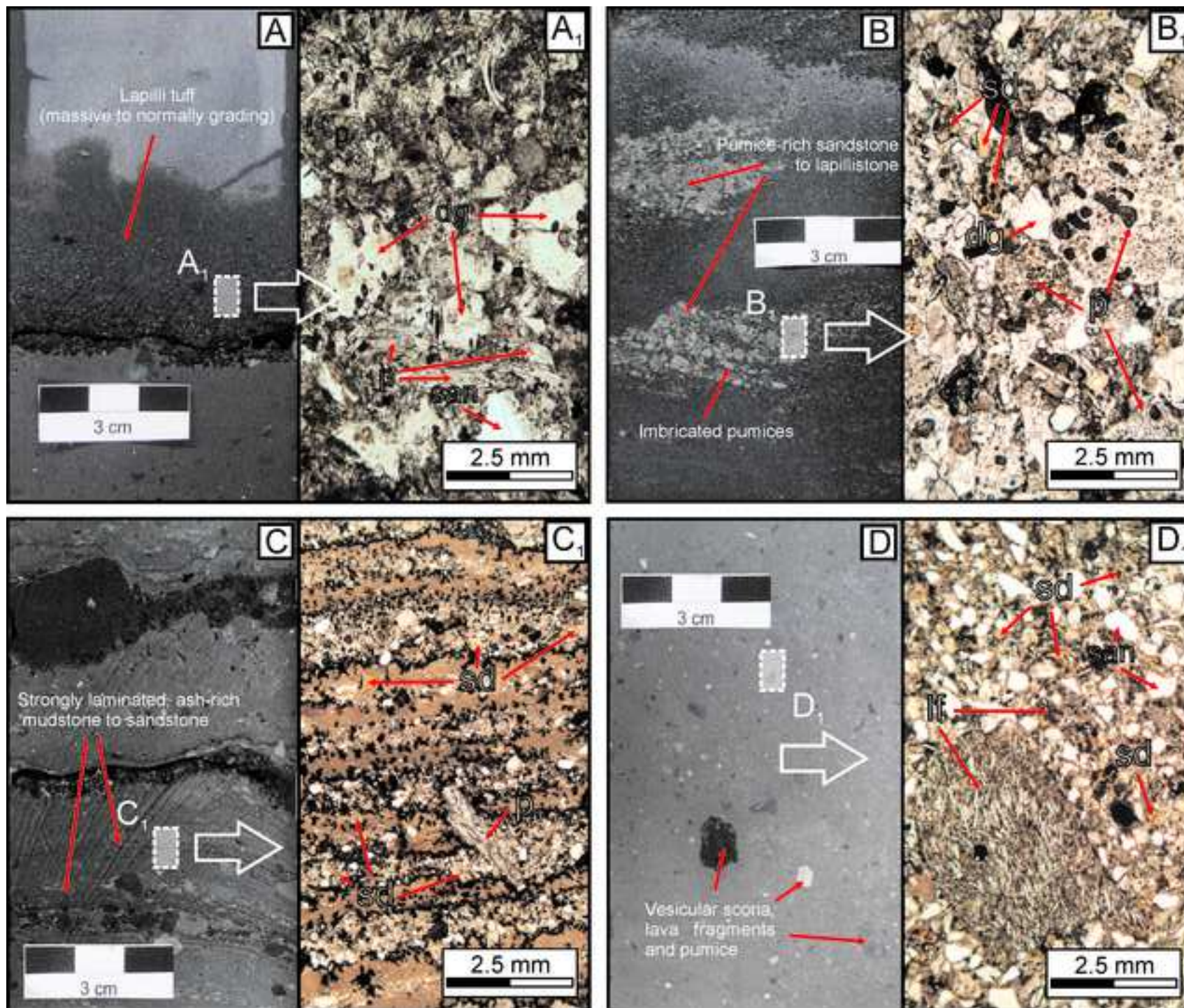


Figure 3
[Click here to download high resolution image](#)

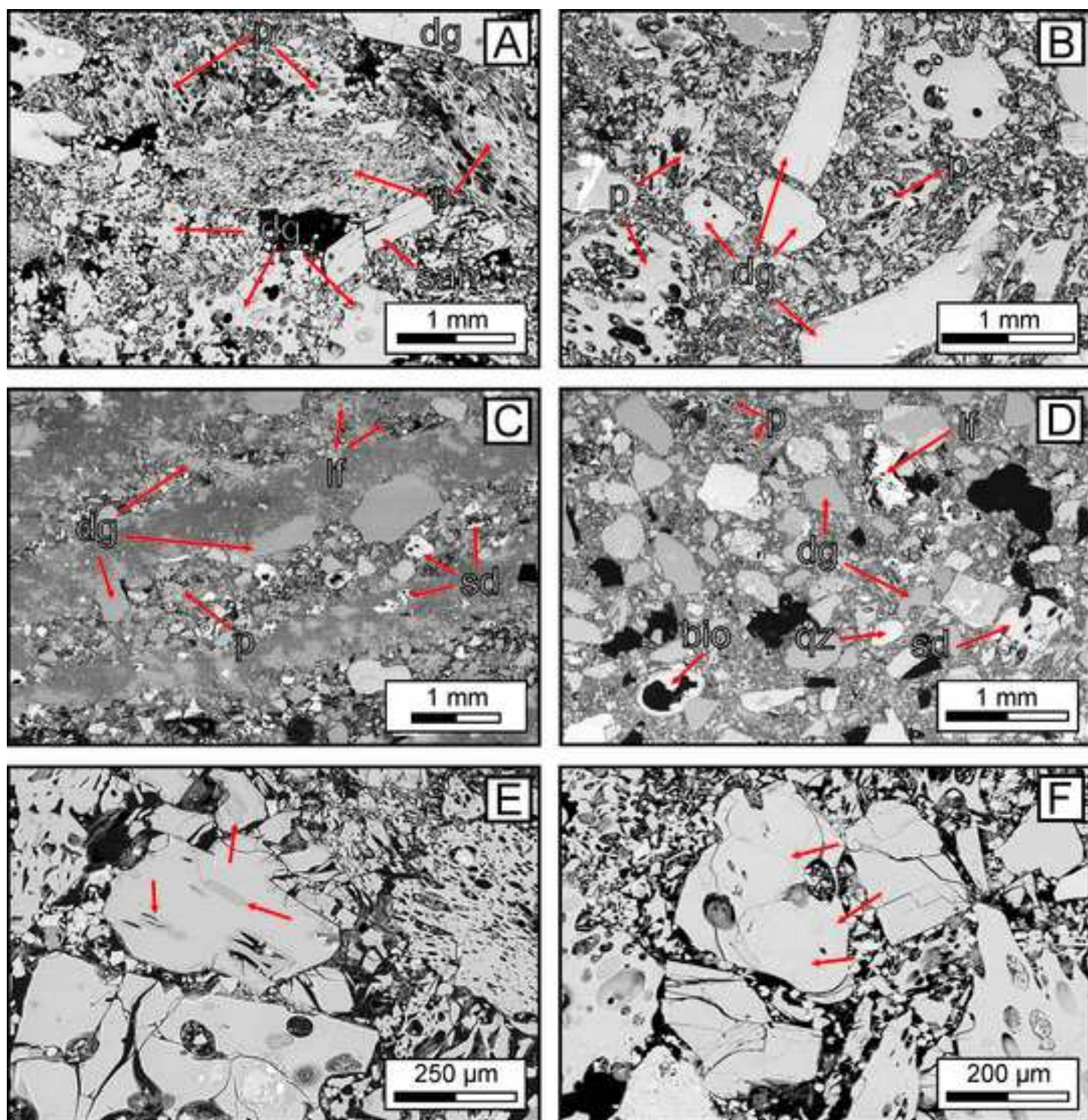


Figure 4
[Click here to download high resolution image](#)

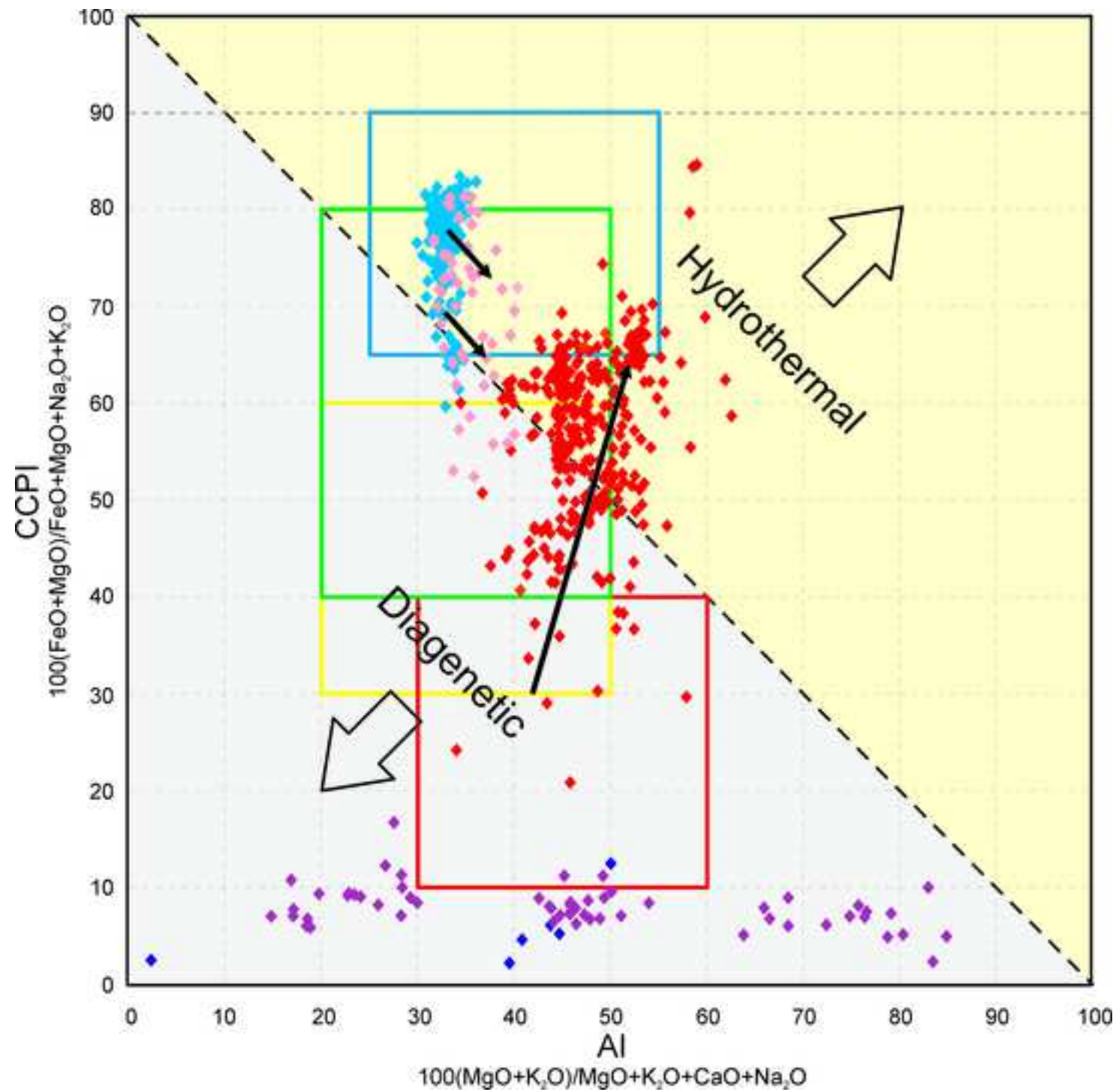


Figure 5
[Click here to download high resolution image](#)

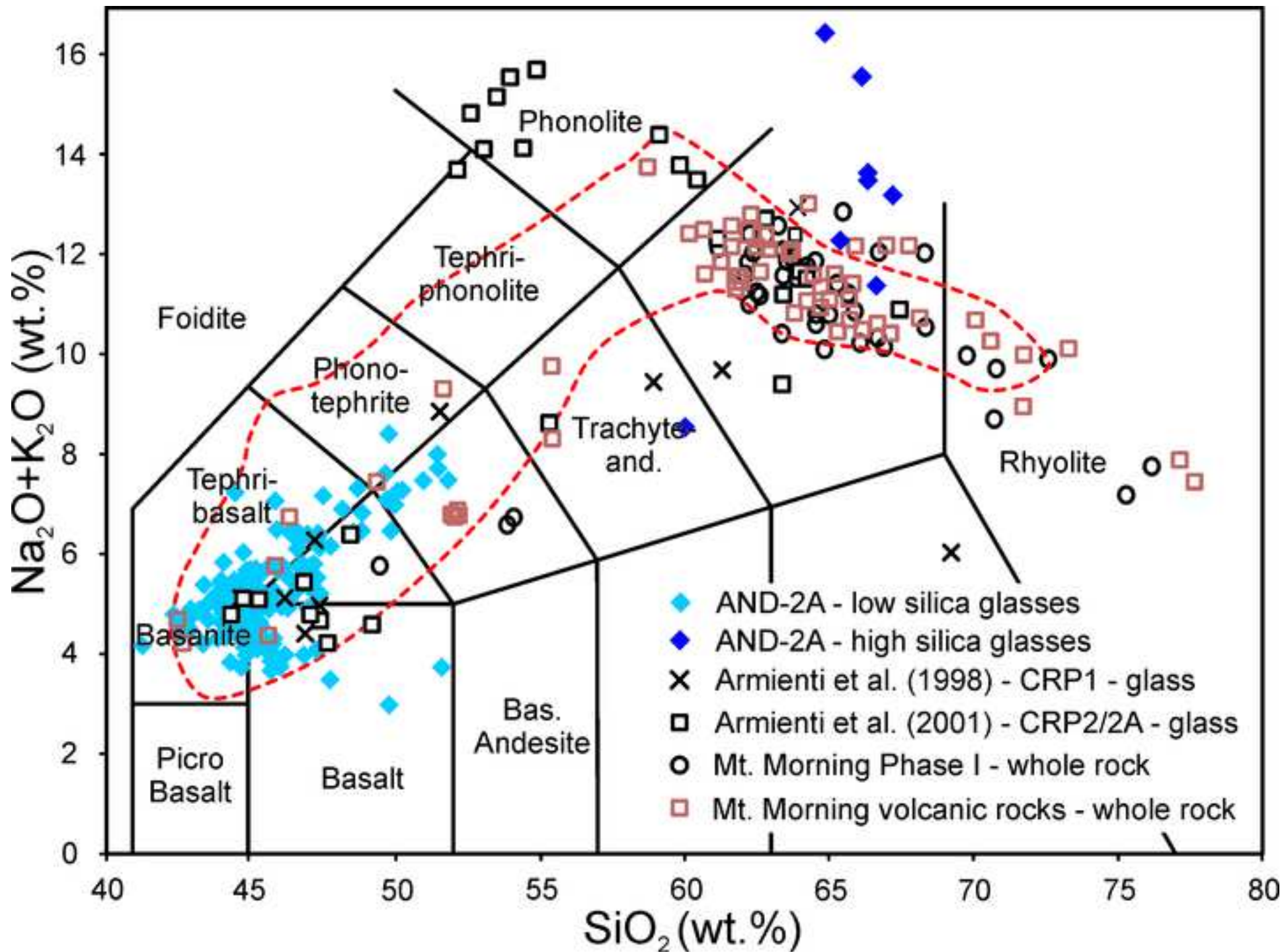


Figure 6
[Click here to download high resolution image](#)

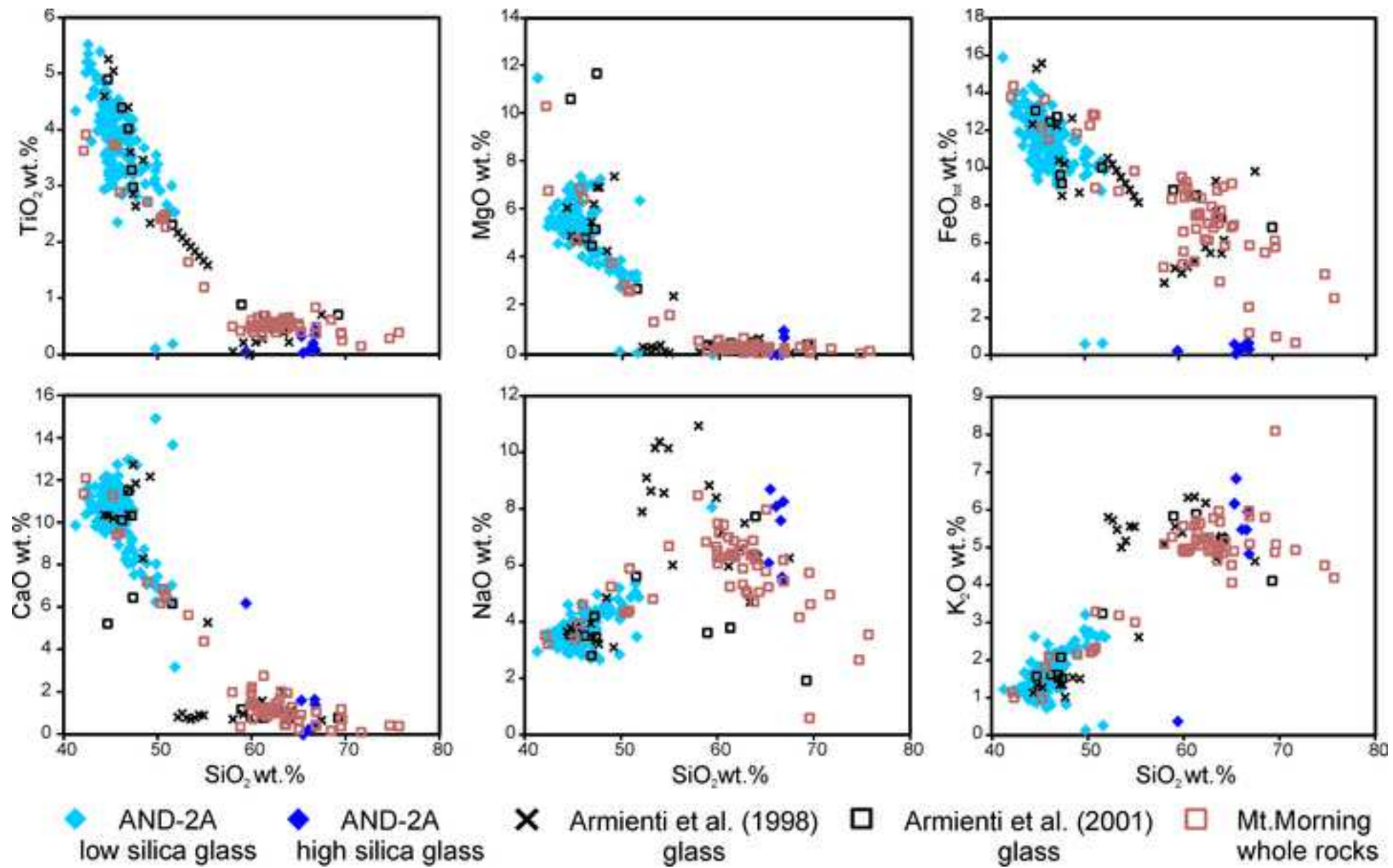


Figure 7

[Click here to download high resolution image](#)

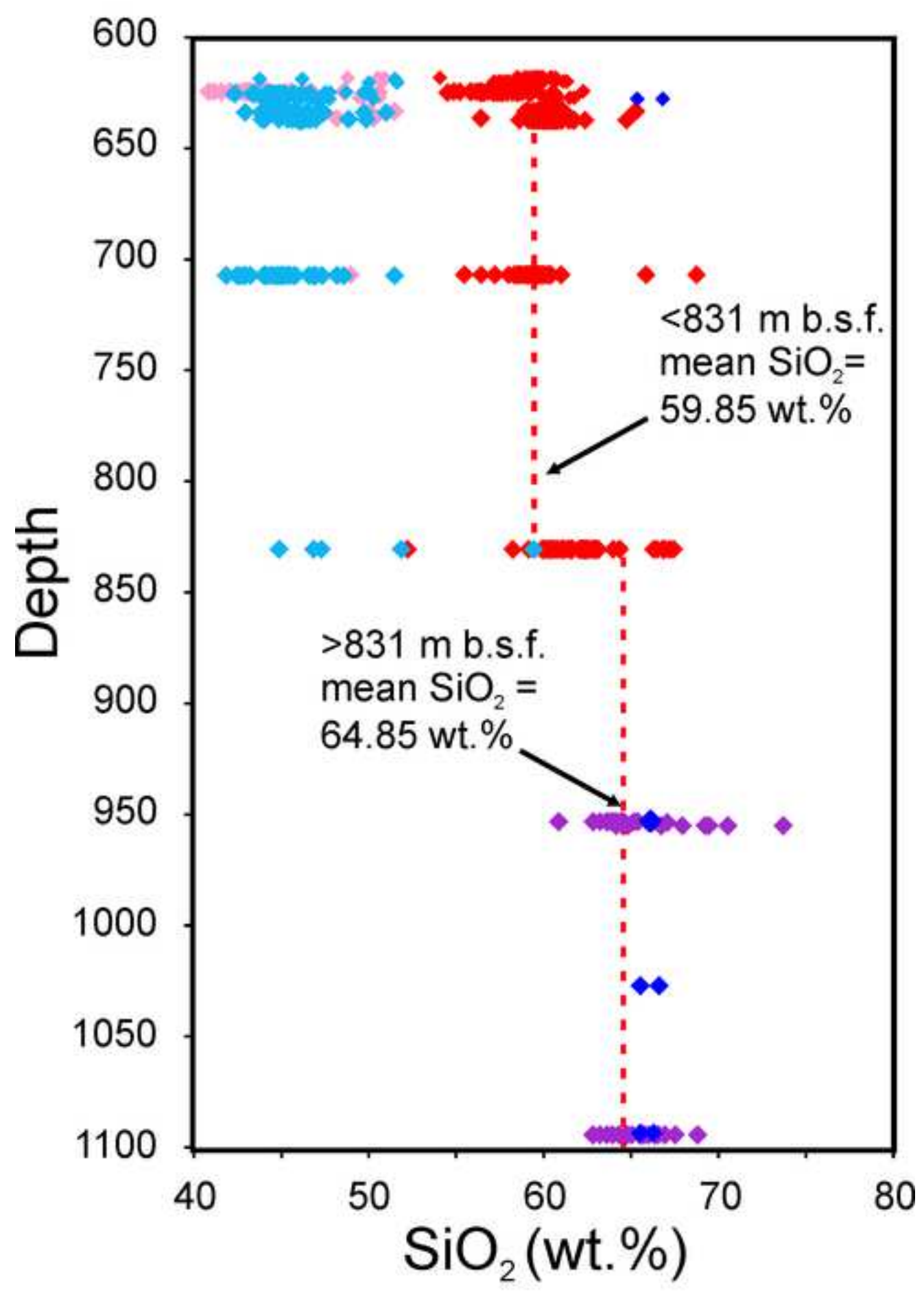


Figure 8
[Click here to download high resolution image](#)

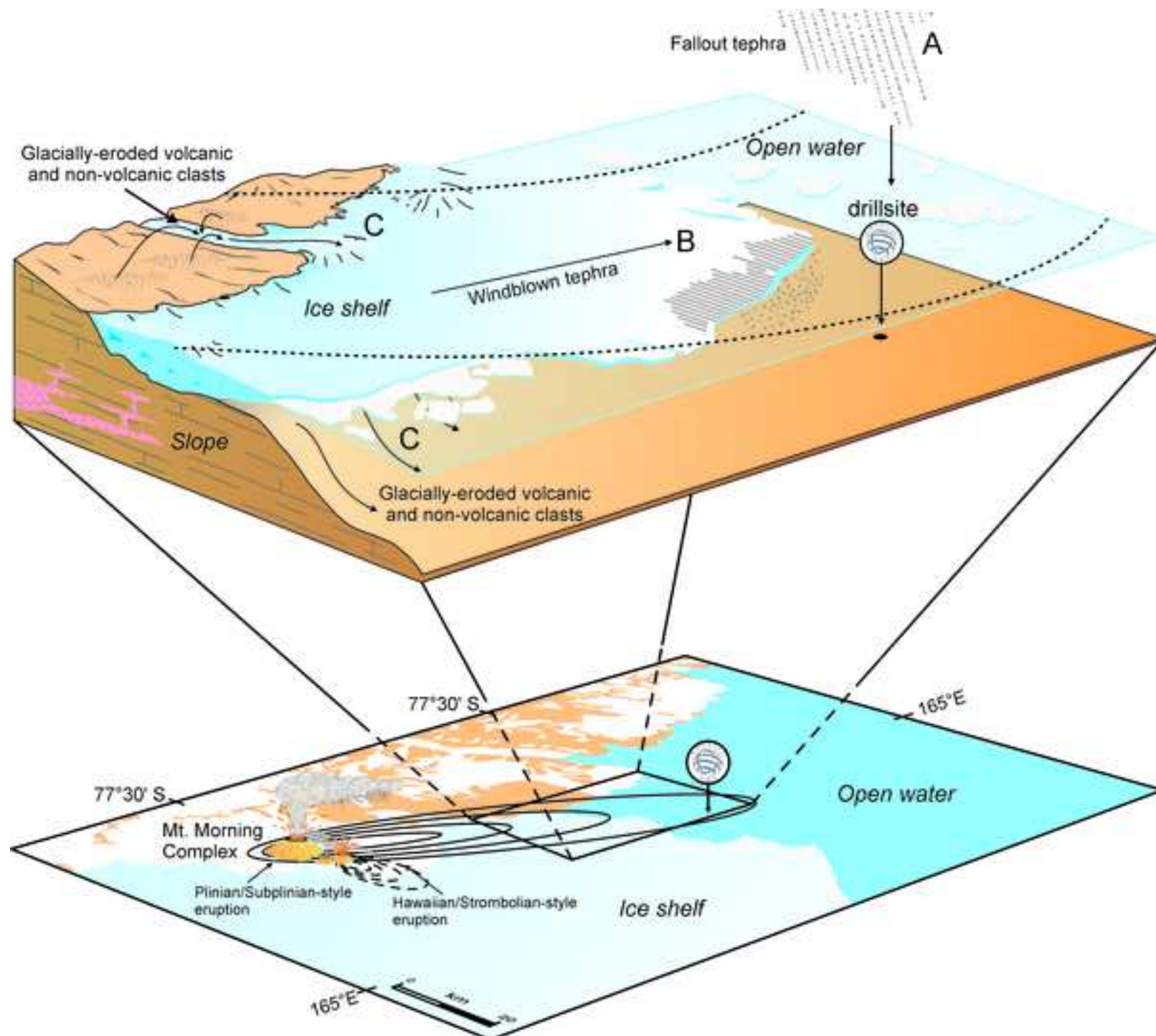


TABLE 1. DESCRIPTION OF ANALYZED SAMPLES

Sample depth	LSU	Age (Ma)	Sediment type	Lithology	Glass composition (unaltered)
AND 2A - 621.24-27	LSU9	17.1-17.39	Resedimented volcanoclastic	Resedimented pumice- and scoria-rich sandstone to lapillistone	Basanite/Mugearite
AND 2A - 622.65-67	LSU9	17.1-17.39	Volcanogenic	Shards-rich siltstone/sandstone	Basanite/Mugearite
AND 2A - 627.27-29	LSU9	17.1-17.39	Volcanogenic	Shards-rich siltstone/sandstone	Basalt/Basanite/Mugearite
AND 2A - 627.46-48	LSU9	17.1-17.39	Volcanogenic	Shards-rich siltstone/sandstone	N/A
AND 2A - 627.85-88	LSU9	17.1-17.39	Volcanogenic	Shards-rich siltstone/sandstone	Basanite/Basalt
AND 2A - 630.14-17	LSU9	17.1-17.39	Volcanogenic	Shards-rich siltstone/sandstone	Basanite/Mugearite
AND 2A - 636.20-22	LSU9	17.1-17.39	Resedimented volcanoclastic	Resedimented, laminated, ash-rich mudstone to sandstone	Basanite/Basalt
AND 2A - 636.23-26	LSU9	17.1-17.39	Resedimented volcanoclastic	Resedimented, laminated, ash-rich mudstone	Basanite/Mugearite
AND 2A - 639.27-30	LSU9	17.1-17.39	Volcanogenic	Shards-rich siltstone/sandstone	Basanite/Mugearite
AND 2A - 640.13-19	LSU9	17.39±0.12 ⁴⁰ Ar/ ³⁹ Ar	Pyroclastic deposit	Lapilli tuff	Basanite
AND 2A - 709.14-16	LSU10	18.15±0.34 ⁴⁰ Ar/ ³⁹ Ar	Resedimented volcanoclastic	Resedimented pumice- and scoria-rich sandstone to lapillistone	Basanite/Basalt
AND 2A - 709.17-19	LSU10	17.93±0.4 ⁴⁰ Ar/ ³⁹ Ar	Resedimented volcanoclastic	Resedimented pumice- and scoria-rich sandstone to lapillistone	Basanite/Basalt
AND 2A - 709.19-21	LSU10	~17.39	Resedimented volcanoclastic	Resedimented pumice- and scoria-rich sandstone to lapillistone	Basanite/Basalt
AND 2A - 831.66-68	LSU11	18.71±0.33 ⁴⁰ Ar/ ³⁹ Ar	Resedimented volcanoclastic	Resedimented pumice- and scoria-rich sandstone to lapillistone	Basanite/Basalt
AND 2A - 953.28-30	LSU12	19.44±0.34 ⁴⁰ Ar/ ³⁹ Ar	Resedimented volcanoclastic	Resedimented pumice- and scoria-rich sandstone to lapillistone	Trachyte
AND 2A - 953.54-58	LSU12	19.49±0.34 ⁴⁰ Ar/ ³⁹ Ar	Resedimented volcanoclastic	Resedimented pumice- and scoria-rich sandstone to lapillistone	Basanite
AND 2A - 954.05-08	LSU12	19.5-20	Resedimented volcanoclastic	Resedimented pumice- and scoria-rich sandstone to lapillistone	N/A
AND 2A - 1027.27-30	LSU13	19.5-20	Resedimented volcanoclastic	Resedimented, laminated, ash-rich mudstone to sandstone	Trachyte
AND 2A - 1093-03	LSU13	20.01±0.35 ⁴⁰ Ar/ ³⁹ Ar	Resedimented volcanoclastic	Resedimented pumice- and scoria-rich sandstone to lapillistone	Trachyte

Note: Age are from Di Vincenzo et al. (2010); N/A - Not Available

Table 2

TABLE 2. CHEMICAL COMPOSITIONS OF ANALYZED VOLCANIC GLASS

Sample	621.24-22		636.20-22		636.23-26		640.13-19		709.14-16		709.17-19		709.19-21		831.66-68		953.28-30		953.56-58		1027.27-30		1093-03	
SiO ₂	43.80	51.50	42.96	46.38	43.86	50.99	46.11	42.86	48.19	42.49	51.48	42.63	48.58	44.90	59.42	66.83	41.29	49.81	66.56	66.24				
TiO ₂	4.16	3.01	3.80	3.24	4.27	2.67	4.27	5.07	3.27	5.21	2.56	5.52	3.68	4.00	0.05	0.08	4.34	0.10	0.19	0.04				
Al ₂ O ₃	15.25	15.35	14.86	16.24	14.83	15.78	15.09	14.55	15.67	13.51	15.88	13.19	13.73	15.93	24.24	18.17	11.73	30.84	18.09	18.55				
FeO	12.49	10.34	11.92	10.15	12.85	10.09	12.33	12.91	10.82	12.89	8.76	13.97	11.45	10.02	0.23	0.31	15.90	0.60	0.61	0.87				
MnO	0.14	0.27	0.19	0.21	0.18	0.15	0.24	0.23	0.23	0.24	0.25	0.28	0.32	0.26	0.00	0.00	0.25	0.00	0.01	0.05				
MgO	5.61	3.36	5.38	4.81	5.54	3.31	5.13	5.62	3.84	5.59	3.11	5.68	4.01	5.86	0.00	0.71	9.87	0.12	0.03	0.03				
CaO	10.87	7.04	10.93	10.23	10.89	6.81	9.87	11.26	7.62	11.15	6.29	11.65	8.73	11.78	6.19	0.44	11.51	14.91	0.33	0.13				
Na ₂ O	3.82	5.04	3.49	4.36	3.83	4.86	4.07	3.43	4.53	3.47	5.35	3.38	4.22	3.77	8.06	8.25	2.95	2.84	7.59	7.56				
K ₂ O	1.35	2.67	1.25	2.08	1.35	2.61	1.70	1.10	2.36	1.14	2.64	1.12	2.21	1.76	0.36	4.82	1.22	0.14	5.47	6.00				
P ₂ O ₅	1.50	1.09	1.56	1.19	1.38	1.18	0.99	1.61	1.42	1.63	1.11	1.65	1.39	0.77	0.00	0.02	0.00	0.01	0.00	0.01				
Total	98.99	99.66	96.32	98.87	99.00	98.45	99.79	98.65	97.95	98.12	98.16	99.06	98.32	99.06	98.86	99.65	99.20	99.38	98.88	99.67				
Alkali	5.17	7.71	4.74	6.44	5.18	7.47	5.77	4.53	6.90	4.61	7.99	4.51	6.43	5.53	8.42	13.08	4.16	2.98	13.05	13.56				

Note: Values shown are the highest and lowest SiO₂ contents within a given sample

Supplemental file

[Click here to download Supplemental file: Supplemental Captions.docx](#)

Supplemental file

[Click here to download Supplemental file: Suppl Figure 1.tif](#)

Supplemental file

[Click here to download Supplemental file: Suppl Table 1.tif](#)